

Air Force Institute of Technology

AFIT Scholar

Theses and Dissertations

Student Graduate Works

3-26-2002

The Horizontal Extent of Lightning Based on Altitude and Atmospheric Temperature

David R. Vollmer

Follow this and additional works at: <https://scholar.afit.edu/etd>



Part of the [Meteorology Commons](#)

Recommended Citation

Vollmer, David R., "The Horizontal Extent of Lightning Based on Altitude and Atmospheric Temperature" (2002). *Theses and Dissertations*. 4501.

<https://scholar.afit.edu/etd/4501>

This Thesis is brought to you for free and open access by the Student Graduate Works at AFIT Scholar. It has been accepted for inclusion in Theses and Dissertations by an authorized administrator of AFIT Scholar. For more information, please contact richard.mansfield@afit.edu.



**THE HORIZONTAL EXTENT OF
LIGHTNING BASED ON ALTITUDE AND
ATMOSPHERIC TEMPERATURE**

THESIS

David R. Vollmer, Captain, USAF

AFIT/GM/ENP/02M-10

**DEPARTMENT OF THE AIR FORCE
AIR UNIVERSITY**

AIR FORCE INSTITUTE OF TECHNOLOGY

Wright-Patterson Air Force Base, Ohio

APPROVED FOR PUBLIC RELEASE; DISTRIBUTION UNLIMITED.

Report Documentation Page

Report Date 26 Mar 02	Report Type Final	Dates Covered (from... to) Jun 01 - Mar 02
Title and Subtitle The Horizontal Extent of Lightning Based on Altitude and Atmospheric Temperature	Contract Number	
	Grant Number	
	Program Element Number	
Author(s) Capt David R. Vollmer, USAF	Project Number	
	Task Number	
	Work Unit Number	
Performing Organization Name(s) and Address(es) Air Force Institute of Technology Graduate School of Engineering and Management (AFIT/EN) 2950 P Street, Bldg 640 WPAFB OH 45433-7765	Performing Organization Report Number AFIT/GM/ENP/02M-10	
Sponsoring/Monitoring Agency Name(s) and Address(es) ASC/YCA ATTN: Lt Col Robert S. Baerst 2690 Loop Road West WPAFB OH 45433	Sponsor/Monitor's Acronym(s)	
	Sponsor/Monitor's Report Number(s)	
Distribution/Availability Statement Approved for public release, distribution unlimited		
Supplementary Notes		
Abstract Lightning poses a threat to aircraft in flight. To mitigate this threat, the U.S. Air Force requested a study of lightning distances. Three-Dimensional lightning data were examined for this study, spanning 1 March 1997 to 31 May 2001 and obtained from the Lightning Detection and Ranging System (LDAR) at the Kennedy Space Center, FL. The LDAR data points were first grouped into lightning flashes and branches using spatial and temporal criteria. Rawinsonde data were vertically interpolated to determine the temperature at the flash source point and each branch end point. The horizontal distance from flash sources to branch end was calculated. Percentiles of branch distance were examined as a function of altitude and temperature of the flash source and branch end points. The longest 99th percentile of branch distance (35 to 40 km) was found at 2 to 7 km altitude and between 10 and -20C. The altitude range of the longest branches remained similar by season, but the longest branches were found in the winter and spring months, with summer and autumn distances shorter by 5 to 10 km. Summer results showed longer branch distances to the south and the winter data showed a significant elongation to the north.		

Subject Terms Lightning, Atmospheric Electricity, Lightning Protection, Electric Discharges	
Report Classification unclassified	Classification of this page unclassified
Classification of Abstract unclassified	Limitation of Abstract UU
Number of Pages 80	

The views expressed in this thesis are those of the author and do not reflect the official policy or position of the United States Air Force, Department of Defense, or the U.S. Government.

AFIT/GM/ENP/02M-10

THE HORIZONTAL EXTENT OF LIGHTNING BASED ON ALTITUDE AND
ATMOSPHERIC TEMPERATURE

THESIS

Presented to the Faculty

Department of Engineering Physics

Graduate School of Engineering and Management

Air Force Institute of Technology

Air University

Air Education and Training Command

In Partial Fulfillment of the Requirements for the

Degree of Master of Science in Meteorology

David R. Vollmer, B.S.

Captain, USAF

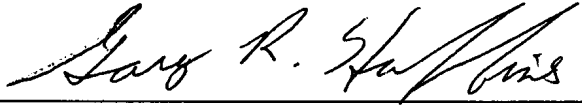
March 2002

APPROVED FOR PUBLIC RELEASE; DISTRIBUTION UNLIMITED.

THE HORIZONTAL EXTENT OF LIGHTNING BASED ON ALTITUDE AND
ATMOSPHERIC TEMPERATURE

David R. Vollmer, B.S.
Captain, USAF

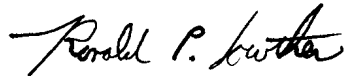
Approved:



Gary R. Huffines (Chairman)

26 Feb 2002

date



Ronald P. Lowther (Member)

26 Feb 02

date



Devin J. Della-Rose (Member)

26 Feb 02

date

Acknowledgments

I would like to express my sincere appreciation to my faculty advisor, Major Gary Huffines, for his expertise, patience, and willingness to help. My other thesis committee members, Lieutenant Colonel Ron Lowther and Major Devin Della-Rose, have contributed to this work through their suggestions and encouragement, and are therefore deserving of my thanks. My research partners and classmates Captain Todd McNamara and First Lieutenant Lee Nelson were indispensable and were responsible for a sizable portion of the computer programming required for my thesis. All of my classmates have offered technical advice and assistance, helping me to improve my work. To my classmates, then, I offer my ceaseless gratitude.

I'd like to thank my sponsors at the U.S. Air Force C-17 System Program Office. Their financial support was invaluable and their enthusiasm for my research was invigorating and inspiring. More thanks go to NASA through whom the massive amounts of lightning data and one of the algorithms came. I'd also like to thank the Air Force Combat Climatology Center and the NOAA Forecast Systems Laboratory for the upper-air data used in this project.

On the home front, I cannot thank my loving wife enough for all of her support and perseverance. While I labored away at my thesis, she was writing her own, yet she still had the time for my concerns. She offered help and advice of a technical nature, but more importantly, she provided the emotional support so critical to such an endeavor. My family and friends have all garnered my gratitude for their unwavering support.

David R. Vollmer

Table of Contents

	Page
Acknowledgments.....	iv
Table of Contents.....	v
List of Figures	vii
List of Tables	ix
Abstract	x
I. Introduction.....	1
1.1 Background	1
1.2 Problem Statement	3
1.3 Research Objectives	3
1.4 Research Impact	4
II. Literature Review	5
2.1 Cloud Charge Structures	5
2.2 The Lightning Flash.....	7
2.2.1 Cloud-to-Ground Flashes	8
2.2.2 Cloud Flashes	9
2.3 Lightning Phenomenology.....	10
2.4 Lightning Detection and Ranging (LDAR)	12
III. Methodology	15
3.1 Scope.....	15
3.2 Data Analysis and Parameterization.....	16
3.2.1 Flash Grouping.....	16
3.2.2 Temperature and Distance Analysis.	18
3.2.3 Branch Counts.....	19
3.3 Statistical Methods	20
3.4 Sources of Error	20
3.4.1 LDAR Error	20
3.4.2 Flash-Grouping Error	21
3.4.3 Branch Distance Error.....	21
3.4.4 Sounding Error.....	21
3.4.5 Temperature Error.....	22

3.4.6 Sampling Error.....	23
3.4.7 Counting Error	24
IV. Results and Analysis	25
4.1 Maximum Horizontal Branch Distances.....	25
4.2 Statistical Distribution of Branch Distances	26
4.3 Percentiles of Branch Distance – Total Period	31
4.3.1 99 th Percentile (Total Period) – Vertical Distributions	32
4.3.2 99 th Percentile (Total Period) – Horizontal Distributions	36
4.3.3 99 th Percentile (Total Period) – Conclusions	36
4.4 99 th Percentile of Distance - Spring	37
4.4.1 99 th Percentile (Spring) – Vertical Distributions	37
4.4.2 99 th Percentile (Spring) – Conclusions	39
4.5 99 th Percentile of Distance - Summer	39
4.5.1 99 th Percentile (Summer) – Vertical Distributions	40
4.5.2 99 th Percentile (Summer) – Conclusions	41
4.6 99 th Percentile of Distance - Autumn.....	42
4.6.1 99 th Percentile (Autumn) – Vertical Distributions	42
4.6.2 99 th Percentile (Autumn) – Conclusions	43
4.7 99 th Percentile of Distance - Winter.....	44
4.7.1 99 th Percentile (Winter) – Vertical Distributions	44
4.7.2 99 th Percentile (Winter) – Conclusions	46
4.8 Summary of Vertical Distributions	46
4.9 99 th Percentile (Seasonal) – Horizontal Distributions	47
V. Conclusions	52
5.1 Conclusions	52
5.2 Recommendations	54
5.2.1 Operator Recommendations	54
5.2.2 Future Research Recommendations.....	55
Appendix A: Percentiles of Distance by Altitude	57
Appendix B: Percentiles of Distance By Temperature	62
Bibliography.....	66
Vita.....	69

List of Figures

	Page
Figure 1. Idealized Cloud Charge Structure in a Thunderstorm.....	6
Figure 2. Evolution of the CG Lightning Discharge	9
Figure 3. Locations and Orientation of LDAR Sites at KSC.....	13
Figure 4. Algorithm Distance Error as a Function of Distance from LDAR.....	17
Figure 5. Grouped LDAR Data – Single Flash.....	18
Figure 6. Maximum Horizontal Branch Distances by Altitude and Temperature	26
Figure 7. Distributions of Branch Counts	27
Figure 8. Frequency Distribution of Horizontal Branch Distances for Branches Ending at 7.2 to 7.5 km Altitude	28
Figure 9. Frequency Distribution of Horizontal Branch Distances for Branches Ending at -10° to -12°C.....	29
Figure 10. Frequency Distribution of Horizontal Branch Distances for Branches Ending at 25.2 to 25.5 km Altitude	30
Figure 11. Frequency Distribution of Horizontal Branch Distances for Branches Ending at 28° to 26°C.....	31
Figure 12. Percentiles of Branch Distance Based on Altitude and Temperature of the Branch End Points.....	32
Figure 13. 99 th Percentile of Branch Distance by Altitude (Total Period).....	33
Figure 14. Frequency Distribution of Horizontal Branch Distances for Branches Ending at 3 to 3.3 km Altitude	34
Figure 15. 99 th Percentile of Branch Distance by Temperature (Total Period).....	35
Figure 16. Frequency Distribution of Horizontal Branch Distances for Branches Ending at 2° to 0°C	35
Figure 17. 99 th Percentile of Distances and Total Branch Counts by Azimuth.....	36
Figure 18. 99 th Percentile of Branch Distance by Altitude (Spring).....	38

Figure 19. 99 th Percentile of Branch Distance by Temperature (Spring)	39
Figure 20. 99 th Percentile of Branch Distance by Altitude (Summer)	40
Figure 21. 99 th Percentile of Branch Distance by Temperature (Summer).....	41
Figure 22. 99 th Percentile of Branch Distance by Altitude (Autumn)	42
Figure 23. 99 th Percentile of Branch Distance by Temperature (Autumn).....	43
Figure 24. 99 th Percentile of Branch Distance by Altitude (Winter)	45
Figure 25. 99 th Percentile of Branch Distance by Temperature (Winter).....	46
Figure 26. 99 th Percentile of Branch Distance by Azimuth for Spring.....	48
Figure 27. 99 th Percentile of Branch Distance by Azimuth for Summer.....	49
Figure 28. 99 th Percentile of Branch Distance by Azimuth for Autumn	50
Figure 29. 99 th Percentile of Branch Distance by Azimuth for Winter	51

List of Tables

	Page
Table 1. Flash and Branch Counts by Year	15
Table 2. Temperature Error by Mandatory Level.....	23
Table 3. 99 th Percentile of Distance by Predictor and Season.....	47

Abstract

Lightning poses a threat to aircraft in flight. In order to mitigate that threat, the U.S. Air Force C-17 System Program Office requested a study of how far lightning can travel from a thunderstorm. To meet this request, three-dimensional lightning data were examined from the period 1 March 1997 to 31 May 2001, obtained from the Lightning Detection and Ranging System (LDAR) at the Kennedy Space Center, Florida.

The LDAR data points were first grouped sequentially into lightning flashes and branches using spatial and temporal criteria. This study examined those branches whose parent flash source point was within 60 km of LDAR. Next, rawinsonde data were linearly interpolated in the vertical to determine the temperature of the flash source point and each branch end point. The horizontal distance from flash source to branch end was then calculated. Finally, percentiles of branch distance were examined as a function of altitude and temperature of the flash source and branch end points. The 99th percentile was studied in depth in order to minimize contamination by extreme outlier distance values. The longest branches were found to occur from 2 to 7 km altitude and between 10° and -20°C. The altitude range of the longest branches remained similar by season, but the maximum 99th percentile branch distance values were found in the winter and spring months (46 to 50 km), with summer and autumn distances found to be shorter (40 to 44 km). Summer results showed longer branch distances to the south and the winter data showed a significant elongation to the north. These results paint a detailed picture of the three-dimensional lightning threat.

THE HORIZONTAL EXTENT OF LIGHTNING BASED ON ALTITUDE AND ATMOSPHERIC TEMPERATURE

I. Introduction

1.1 Background

Lightning has posed a threat to aircraft since the inception of human aviation. Aircraft in flight typically attempt to avoid thunderstorms, whenever possible, due to the variety of threats associated with them such as turbulence, hail, and lightning. Lightning strikes can cause physical damage to aircraft surfaces, internal damage to the avionics, and even fuel ignition in rare cases. Most aircraft have electrical grounding systems on board designed to minimize the damage caused by such a strike, but strike avoidance is preferable to damage control.

The U.S. Air Force (USAF) C-17 Globemaster III airlifter is one of the newest aircraft in the service's inventory. In an effort to stem potential lightning damage to this important aircraft, the USAF endeavored to enforce a margin of safety from thunderstorms. In fact, for some time, the USAF was telling its C-17 crews to avoid thunderstorms by 50 nautical miles (T. Krogh 2000, personal communication). This was soon realized to be difficult, especially considering that many of these aircraft fly in and around the southeastern U.S. where summertime thunderstorms are common. In an Interim Safety Supplement (Department of the Air Force 2001) dated 17 July 2001, the USAF discussed the lightning threat. It stated that commercial aircraft strike data indicated that 90% of aircraft lightning strikes occurred in clouds, within 10°C of the

freezing level, and below 23,000 feet; and, that only 55% of strikes to aircraft occurred when thunderstorms were reported “in the vicinity or general area of the aircraft’s position.” The safety supplement then went on to define what the USAF considered to be the “danger area” for in-flight lightning strikes, stating that “areas of high lightning strike potential are defined as when the aircraft is within +/- 10 degrees C Static Air Temperature (SAT) of the freezing level and in clouds (including debris clouds) or in precipitation (including snow).” In other words, lightning can most often be expected from precipitation and clouds from -10° to 10°C, appearing as green, yellow, or red on the aircraft weather radar display. As for what aircrews should do to avoid lightning, the supplement stated: “Aircrews should attempt to avoid high lightning strike potential areas, but may climb or descend through these areas in order to depart or arrive at an airfield.” Therefore, the threat is not limited to cruising altitude alone. The supplement continued: “When approaching or departing airfields where thunderstorms are occurring or are forecast, continue to follow existing guidance for maintaining ... 5 NM [nautical mile] separation from heavy rain showers.”

The first question that logically follows is: how far does lightning travel from a thunderstorm? Additionally, does this distance vary depending upon factors such as flight level or outside air temperature? This study was initiated to answer these questions within the constraints of available three-dimensional lightning data. The primary push behind this investigation came from the USAF, whose complex and sensitive aircraft systems sometimes have particular vulnerabilities to lightning strikes, though these results are more broadly applicable to all general aviation interests. The goal was to determine the nature of the lightning threat to aircraft in flight by determining the

horizontal extent of total lightning activity in thunderstorms, and upon what factors that distance depends.

1.2 Problem Statement

A problem without a solution is not a problem, but rather a constraint. That certainly seems the case here. The problem addressed is one of lightning/aircraft interaction, a situation that rarely has a positive outcome. The USAF wants to know how close to a thunderstorm its aircraft may fly and be reasonably safe from a naturally occurring (not aircraft-induced) lightning flash. The C-17 Globemaster III System Program Office (SPO) requested this study, but much broader issue affecting all USAF aircraft is that lightning can pit aircraft surfaces, which can result in degraded performance and the need for costly repairs. This makes the lightning distance issue not a problem to be solved, but a constraint to be understood and a threat to be mitigated. In summary, the problem was to determine the horizontal distance lightning travels as a function of its altitude and the atmospheric temperature at specific levels.

1.3 Research Objectives

The primary objective of this thesis was to determine the horizontal extent of total lightning in thunderstorms. The data were received from the Lightning Detection and Ranging (LDAR) system operated by the National Aeronautics and Space Administration (NASA) at Kennedy Space Center (KSC), FL. More specifically, the research sought to find relationships between horizontal lightning channel lengths and their altitudes and temperatures.

The predictors examined for lightning flash distances were the altitude and estimated temperature at the flash source point, and the altitude and estimated temperature at each branch end point. Branch counts were examined for each of these four vertical predictors. The objective was to find the altitude and temperature at which an aircrew might expect the longest lightning flashes and the highest threat. Additionally, the azimuth of each branch was examined at various levels along with branch count with the purpose of finding a directional preference for lightning distance and frequency.

1.4 Research Impact

It is hoped that this research will result in a better understanding of where the greatest lightning threat lies. Knowing the distance and count distributions of flashes and branches in the vertical and horizontal, while not a guarantee of safety, will allow aircrews and planners to make more informed decisions about lightning avoidance. This information will then permit the user to weigh more accurately the lightning risks against the necessity of the flight or flight route.

The C-17 SPO will not be the only beneficiary of an analysis of lightning distances. The study that follows will be of value to all aviation interests, since the threat from naturally occurring lightning is not specific to any one airframe or weapon system. Also, since these data come from the KSC, space vehicle and launch safety may be enhanced via these results.

II. Literature Review

2.1 Cloud Charge Structures

Traditionally, thunderstorms have been described as dipoles or tripoles, referring to the vertical distribution of charge within the cloud. The tripolar structure is described in detail by MacGorman and Rust (1998) and is characterized by a main negative charge at mid-levels with a positive charge above and a smaller positive charge below it. The dipole model is representative of those storms lacking the lower positive charge.

MacGorman and Rust offer a further modification to the dipole/tripole model. Evidence exists of a screening layer of charge opposite to that inside the cloud along the upper boundary. For a positive upper charge, the screening layer would be negative.

Stolzenburg et al. (1998) showed a more complex electrical structure of thunderstorms by examining individual cells, Mesoscale Convective Systems (MCSs), and supercell storms. Surprisingly, the different thunderstorm types tended to show a similar basic charge structure (Figure 1). The main differences were in the temperatures (and therefore relative altitudes) of the charge regions.

Stolzenburg et al. (1998) found that the average main negative charge center from nine electrical soundings taken in isolated New Mexico thunderstorm updrafts had an altitude of 6.05 km and a temperature of -7°C . The 11 MCS updrafts from the southern Great Plains had an average main negative charge center at 6.93 km and -16°C . Lastly, the strong updrafts of 7 supercells, also on the Great Plains, showed a main negative charge center at 9.12 km and -22°C . A direct dependence of charge region height upon updraft speed was found. Faster updrafts tended to lead to higher and colder charge

centers. When averaged across all of the electrical soundings in the study, the correlation was less than it was within the individual categories, but still managed to show at a 95% confidence level that each m s^{-1} increase in updraft speed would move the main negative charge center up by an average of -1°C .

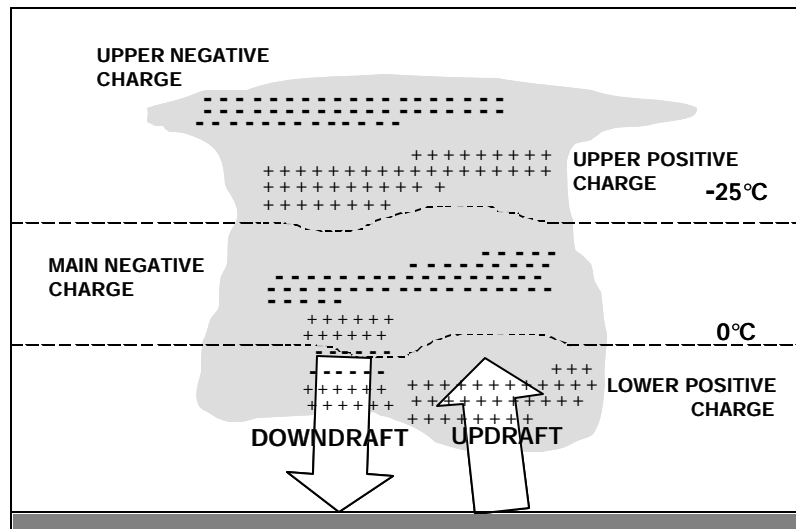


Figure 1. Idealized Cloud Charge Structure in a Thunderstorm. There are four distinct charge regions within the updraft region, and up to six distinct charge regions outside the updraft (adapted from Stolzenburg et al. 1998).

The implications of this on the present study are that thunderstorm type may influence the locations of charge regions, and therefore the location of lightning sources, and that non-updraft charge structures may give rise to additional lightning sources. Thunderstorm type is not readily gleaned from the raw LDAR data and is beyond the scope of this study. Deciding specific thunderstorm type may be beyond the abilities of either aviation forecasters or aviators themselves when examining the in-flight lightning risk.

Krieder et al. (1996) examined the electrical structure of Florida thunderstorms using LDAR. Their results showed that cloud-to-ground (CG) flashes tended to cause

electrical field changes where temperatures ranged from -10° to -20°C (at an altitude of 6 to 8 km). Electrical field changes associated with intracloud (IC) flashes (flashes starting and ending in the same cloud) occurred above and below this region, directed toward the center. The results of the present study tend to agree with these findings in that a large number of flashes with near zero horizontal extent were found at these levels.

2.2 *The Lightning Flash*

The Glossary of Meteorology (GOM) defines lightning as a “transient, high-current electric discharge measured in kilometers (Glickman 2000).” Somewhat more detailed is the GOM definition of the lightning discharge, which it defines as:

The series of electrical processes taking place within 1 s by which charge is transferred along a discharge channel between electric charge centers of opposite sign within a thundercloud (intracloud flash), between a cloud charge center and the earth’s surface (cloud-to-ground flash or cloud-to-ground discharge), between two different clouds (intercloud or cloud-to-cloud discharge), or between a cloud charge and the air (air discharge) [parenthetical comments contained in original passage].

The 1 s criterion contained in the definition gives one a feel for the rapidity of the lightning process, and played a role in the temporal logic included in the algorithms in Chapter III.

Lightning flashes are often characterized as either CG flashes or cloud flashes. Hereafter, a cloud flash will refer to any flash not going to ground. While all lightning flashes are similar, there are some characteristics unique to CG flashes. CG flashes will be treated first, followed by a description of cloud flashes, bearing in mind that the distinction between the two is not a discrete boundary but blurred by their physical similarities.

2.2.1 Cloud-to-Ground Flashes. Most descriptions of the lightning flash process begin with CG flashes, probably because they are the most familiar to us. Additionally, CG flashes pose a threat to people and objects on the ground, the realm of most human activities. The discharge process begins when the electric field exceeds the dielectric breakdown value of the air. Lightning initiation usually occurs when this field strength is on the order of 200 kV m^{-1} (Phelps 1974). Once the dielectric breaks down, the stepped leader begins its descent from the base of the cloud. The leader is a highly ionized channel of plasma. The largely invisible stepped leader (Figure 2a - 2e) does not descend in one smooth stroke, but rather in discrete segments (i.e., steps), each about 50-100 m long and $1 \mu\text{s}$ in duration, with roughly 30-50 μs between steps. Typical stepped leader velocity is about $2 \times 10^5 \text{ m s}^{-1}$ (Bergen and Vogelsanger, 1966). Stepped leader propagation has a significant bearing on LDAR accuracy and performance. Once the stepped leader approaches within a few tens of meters of the ground, the attachment process begins, whereby a discharge is induced from the ground (Figure 2f). When this discharge meets the stepped leader, the first return stroke is initiated. The return stroke is a continuous stream of electrons, which illuminates the entire channel (Figure 2g - 2h). In the negative CG flash, a net transfer of electrons is lowered to the ground, whereas a positive CG flash deposits electrons in the cloud.

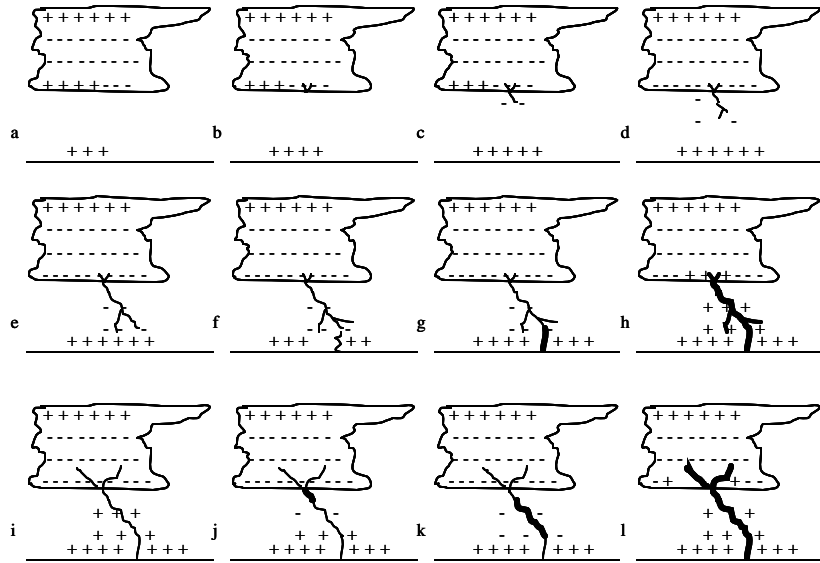


Figure 2. Evolution of the CG Lightning Discharge. Process includes the stepped leader descent (a-e), the attachment process (f), the first return stroke (g-h), the first dart leader (i-k), and the first return stroke (l) (adapted from Uman, 2001).

In many cases, additional charge is available within the cloud at the top of the lightning channel, so successive leaders may descend, known as dart leaders (Figure 2i – 2k). Dart leaders are continuous, and follow the established plasma channel. Each dart leader triggers a separate return stroke (Figure 2l). A single flash may contain several return strokes, each separated by tens of milliseconds (Uman 2001).

2.2.2 Cloud Flashes. Cloud flashes seem to have escaped the same degree of scrutiny applied to CG flashes, primarily because the threat they pose is limited to aviation interests. The electrical field changes produced by the discharge are smoother and slower in a cloud flash than the rapid changes with a CG flash (due to the CG return stroke). The duration of a cloud flash is also usually the same, on the order of 1 s. A primary difference between cloud flashes and CG flashes is the absence of the large return stroke in the former (Uman 2001).

Cloud flashes are basically leaders, physically related to the stepped and dart leaders of the CG stroke in current, waveform, and propagation. Again, cloud flashes do not initiate the massive electromagnetic wave of the CG return stroke, but they are thought to produce recoil streamers, which are weaker cousins to the CG return stroke. In fact, the cloud flash is mechanically very similar to the stepped-leader/first return stroke combination in a CG flash (Ogawa and Brook, 1964). Measurements of propagation speeds, current, and path lengths vary widely from study to study, and this variation complicates understanding of the subject somewhat. IC flashes remain within a single cloud and occur between different charge regions, either by upward propagating leader from the negative region or downward leader from the positive region (Uman 2001). Cloud-to-air discharges, also known simply as air discharges, propagate away from the thunderstorm into the surrounding air (MacGorman and Rust 1998). The cloud-to-cloud flash, also known as the intercloud flash, propagates from the charge region of one cloud to the opposite charge region of another. Importantly, research thus far has not shown significant differences between the characteristics of the three types of cloud flash (Uman 2001).

2.3 Lightning Phenomenology

Overlaying radar imagery with lightning data suggests that the vast majority of lightning flashes occur within 10 km to 20 km of deep convective precipitation, defined as precipitation reaching the surface and extending several kilometers above the freezing level (Engholm et al. 1990). Several limited studies have investigated lightning distances using the same type of three-dimensional lightning data used in this study. One flash

studied over Oklahoma was over 65 km long (Krehbiel et al. 1999). Another study showed an average horizontal channel length of 9.8 km, plus or minus 3.6 km (MacGorman and Rust 1998). Considerable variation in channel length has been found, which plays a major role in this study.

Larouch et al. (1996) found that most of the horizontal cloud discharges over Florida originated between 5 and 7 km altitude, corresponding to -2° to -13°C , which is where the negative charge region typically occurs. Vertical IC flashes were found between 7 and 12 km altitude (-13° to -52°C), presumably between the upper and lower charge regions. Lastly, more horizontal flashes were found from 12 to 20 km altitude (-52°C to the tropopause), in the region typically occupied by positive charge. These discharges were detected by the Very High Frequency (VHF) signals of their recoil streamers. Shao and Kreibel (1996) verified the horizontal nature of cloud discharges within the lower negative region and also in the positive upper region in a separate study over New Mexico.

This research encompasses total lightning, meaning both CG and cloud flashes. How much of each type of lightning would we expect to see in a thunderstorm? Prentice and Mackerras (1977) found a latitudinal relationship, with the ratio of cloud to CG flash increasing with decreasing latitude, varying from 6 at the equator to 2 at 60° latitude. The empirically derived formula they proposed is:

$$z(I, T) = (4.16 + 2.16 \cos(3I)) \left[0.6 + \frac{0.4T}{72 - 0.98I} \right] \quad (1)$$

In (1), z is the ratio of cloud to CG flashes, I is the latitude, and T is the number of thunder days. For this study, the latitude is $28^{\circ} 32' \text{ N}$ (Lennon and Maier 1991).

Additionally, KSC experiences thunderstorms on an average of 75 days per year (Maier et al. 1996). The Operational Climactic Data Summary (OCDS) for Cape Canaveral Air Force Station from the Air Force Combat Climatology Center (AFCCC) shows 87 days of thunder per year, but the above formula is for use when T is less than or equal to 84. Using the T of 75, this formula gives an expected value for the ratio of cloud flashes to CG flashes for this study of 5.5. While discharge type was not determined from the data, it is useful to know that the vast majority of the flashes in the study were likely to not have gone to ground.

2.4 Lightning Detection and Ranging (LDAR)

LDAR is a three-dimensional lightning mapping system located at KSC, and is operated by NASA. The location along Florida's Space Coast is ideal for lightning study, given the sensitive nature of space launch operations conducted at KSC. LDAR is one of the few systems capable of detecting total lightning and reporting its location in three dimensions. It does this using an array of seven VHF radio receivers on 5 m tall antennas with logarithmic radio frequency detectors. The difference in the time of arrival (DTOA) is correlated between stations to determine the location and timing of each signal (Lennon and Maier 1991). The arrangement of the sites is shown in Figure 3.

The current configuration of LDAR allows it to "listen" in two frequency bands. The first band filter chosen was $63 \text{ MHz} \pm 3 \text{ MHz}$, for the convenient reason that this corresponds to local television channel 3, which is not used as a television station for 160 km around LDAR. Later, a second operating band filter, $225 \text{ MHz} \pm 3 \text{ MHz}$, was added, giving LDAR a total operating frequency range of 60 to 300 MHz.

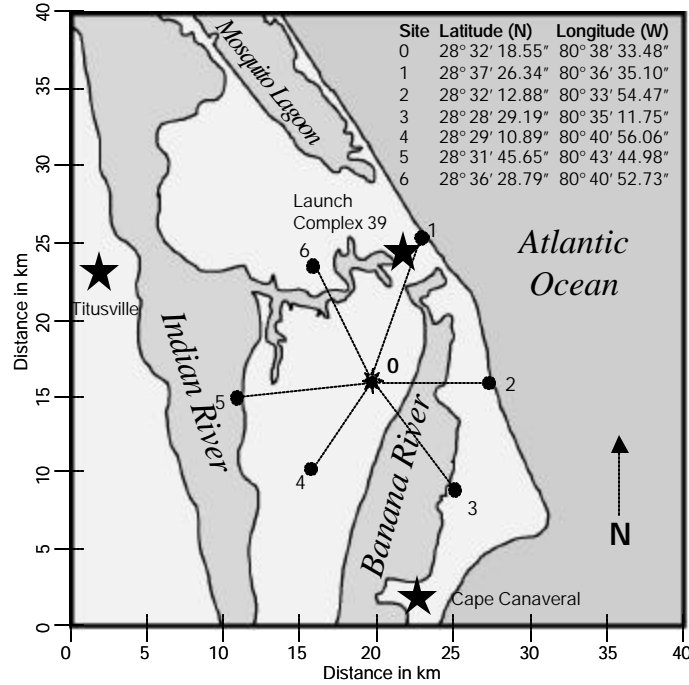


Figure 3. Locations and Orientation of LDAR Sites at KSC. Figure adapted from Lennon and Maier 1991.

In order for a lightning flash to be detected by LDAR, its VHF broadband signal must exceed a threshold value and be detected by the LDAR central site (Site 0 in Figure 4). When such an event is detected at Site 0, the system pauses 100 μ s while it determines the time-of-arrival of the pulse at each of the remote sites, and then determines the time to the nearest microsecond and the 3-D position of the signal. Re-arming of the system takes another 10 μ s. A degree of redundancy is built into the system; System 1 consists of Sites 0, 1, 3, 5, and System 2 is made up of Sites 0, 2, 4, and 6. Both systems work simultaneously. Each of the six remote sites transmits its information to the central site via microwave line-of-sight. The central site has a different receiver and line for each site, as well as its own receiver, all of which funnel into the Pulse Detection and Timing Unit. Timing is done via the Global Positioning System, and data can be displayed in a variety of ways (Lennon and Maier 1991).

There are some sources of error inherent in the LDAR design, not the least of which is the fact that much can happen in the 110 μ s window after LDAR is triggered but is not “listening” for any other signals. This is especially true on active days when several flashes may be propagating simultaneously. LDAR has a range of 250 km, though location error increases with increasing distance from LDAR. Parameterization of this location error will be discussed in Chapter III. Specifically, over KSC, LDAR was found to have an error of 0.5 km with a 93% flash detection efficiency (Maier et al. 1996). Locations of sources detected at 60 km from the LDAR Site 0 can be anywhere along a radially oriented axis 1 km long. Important to CG flash detection and location is the fact that since the LDAR antennas are all on roughly the same plane, vertical location of flashes near the ground is degraded (Murphy et al. 2000).

III. Methodology

3.1 Scope

The data encompassed the time period from 1 March 1997 to 31 May 2001. Upper-air soundings from Cape Canaveral Air Force Station (AFS), FL were used from the same time period to provide temperature data. Some drawbacks of this method are the geographic separation between the LDAR system and the Cape Canaveral AFS rawinsonde launch site (discussed in Section 3.4.4) and the inability of a synoptic sounding to measure the finer-scale temperature structure of a thunderstorm (Section 3.4.6).

Only flashes originating within 60 km of LDAR Site 0 were used. The reason for this was that beyond 61 km, the vertical error of the signal location owing to earth curvature effects exceeds the 300 m vertical bin size used in the branch counting (Boccippio et al. 2001). Over 1 million flashes with nearly 40 million branches were studied. Only those days with both lightning data and sounding data available were included in the study. Eventually, 3531 soundings were used. The breakdown of flashes and branches by year is shown in Table 1.

Table 1. Flash and Branch Counts by Year. Data is for flashes originating within 60 km of LDAR central site.

Flash and Branch Counts by Year			
Period	Days w/ Data	Flash Count	Branch Count
Mar - Dec 1997	206	318,321	15,005,610
Jan - Dec 1998	213	214,366	8,328,293
Jan - Dec 1999	194	241,305	8,690,583
Jan - Dec 2000	166	216,056	6,191,244
Jan - May 2001	62	49,808	1,540,752
Totals	841	1,039,856	39,756,482

3.2 Data Analysis and Parameterization

The original LDAR data consist of the date/time group to the nearest microsecond of each VHF source, as well as the x, y, and z distances in meters to the signal from Site 0. At this point, no information is included to indicate which points belong to which flash or which branch.

3.2.1 Flash Grouping. The LDAR data were grouped according to the algorithm developed by NASA (2001) and described by Murphy et al. (2000). The original program, written in the C program language, was translated into Interactive Data Language (IDL) format. Some modifications were made to the program in order to speed processing time, such as reading in the LDAR files 10,000 lines at a time, but the basic algorithm was left unchanged. Data were assigned a sequential flash number and branch number based on temporal and spatial criteria specified in the original code.

The program first looked at all data points within 3 seconds of the point being considered. The first point in a flash was considered to be the flash source. In order to be included in the current (active) flash, a successive point must have occurred within 0.5 seconds of any point in the active flash. At least one active flash point must have fallen within an ellipsoidal region centered on the point in question whose dimensions are specified by the distance from LDAR and the error associated with that distance. The semi-major axis was roughly radial and included the range error as a function of distance from the central site and altitude (Figure 4), while the semi-minor axis was based in the azimuthal error, also a function of distance from Site 0. If the point failed either the time (0.5 second) or distance (ellipse) criteria, it was considered to be the start of a new flash. To be included in an active branch, a point must have been within 0.03 seconds of any

point in that branch and have met a distance criterion. That criterion was a 1 km radius within 40 km of Site 0, or beyond 40 km by 1 km plus the range over 40 km as depicted in Figure 4. The branch algorithm encompassed a circular area rather than an ellipsoid for all distances and altitudes (Murphy et al. 2000). Any single-point flashes were not assigned a flash number. A grouped flash is found in Figure 5, which shows a three-dimensional depiction of the VHF signal locations detected by LDAR. It appeared to be a cloud flash branching both northward and southward between 5 and 6 km in altitude. Single point flashes were not assigned flash numbers, as they would have no distance information required for this study. LDAR calibration data was also discarded in accordance with the NASA criteria.

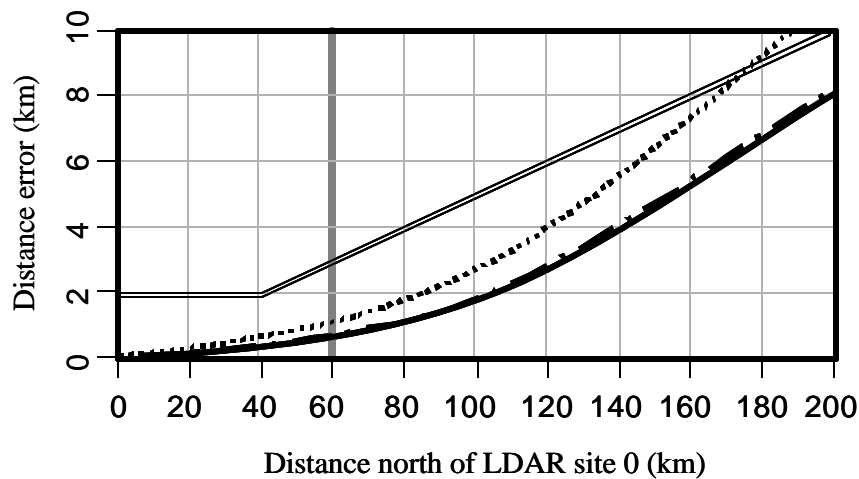


Figure 4. Algorithm Distance Error as a Function of Distance from LDAR. Branch error is indicated as a double line. Also included are the flash grouping ellipsoid semi-major axis at 2 km altitude (dashed), 5 km altitude (solid), and 10 km altitude (dot-dashed). The heavy vertical line indicates the maximum distance for flash source points used in this study (adapted from Murphy et al. 2000).

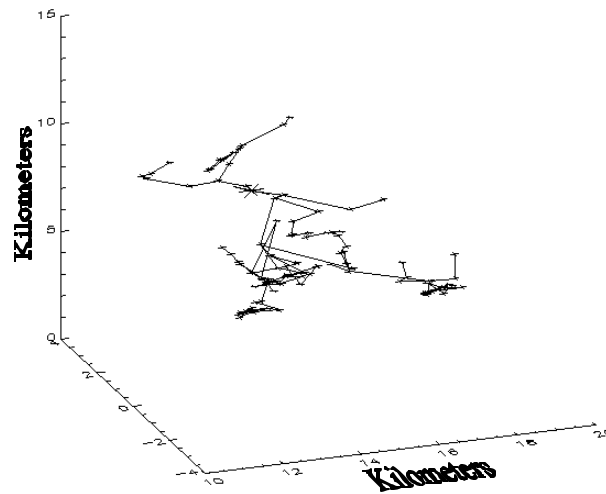


Figure 5. Grouped LDAR Data – Single Flash. The flash was initiated at 3:25:15.634603 UTC 20 March 2001. North is toward the rear and east is toward the right.

3.2.2 Temperature and Distance Analysis. Once the data were grouped, they were further analyzed for horizontal channel length and temperature. For each day of grouped LDAR data, Cape Canaveral AFS (KXMR) sounding data were opened for all soundings that day, the day prior, and the day after. Temperature and altitude information were read from these files and interpolated into an array of temperatures. The array width was determined by the number of soundings available over the 3 day period. The array length was 170 lines, at 150 m increments, starting at 150 m. This interval was chosen to correspond to approximately 1°C from a standard US atmospheric lapse rate of $-6.5^{\circ}\text{C km}^{-1}$ (Bluestein 1992), or one-half of the chosen acceptable error limit for this study of 2°C . The 2°C resolution corresponds in turn to roughly 1000 ft, again in a standard US atmosphere. If a relationship were to be found between atmospheric temperatures and strike threat, aircraft could be given 1000-foot altitude changes to minimize that threat. The altitude versus distance tables (Table A-1 and Table

A-2) in Appendix A have roughly 1000 feet between intervals. Over the duration of the study the average atmospheric lapse rate was determined to be $-6.665^{\circ}\text{C km}^{-1}$, so the US standard atmosphere assumption was reasonable for determining desired altitude increments.

The maximum altitude allowed was 25.5 km, above which LDAR data was discarded. The reasoning for this is that the vast majority of LDAR data occurred below this level, yet most soundings ended near or above this level. If a sounding ended below 25.5 km, data from the next nearest sounding with available data was transferred to that part of the array. On some occasions, this caused a nighttime sounding to be mixed with a daytime sounding. The error associated with the change in temperature between soundings at the same level is described in detail in Section 3.4.5.

3.2.3 Branch Counts. The next step was to find some common information from the 841 daily files. Each line in a file contained all of the time, location, and temperature information of the flash source location and the branch end point for that line, as well as the distance between them. Since lightning flashes often contain on the order of tens of individual branches oriented in several directions, it was important to look at each branch rather than just the longest branch. To accomplish this, the branches were counted according to their horizontal distance from flash source points to branch end points, the vertical location of the branches, and the compass direction from flash sources to branch end points. Each branch was then treated as if it were a single channel flash, starting at the parent flash source point (not necessarily where the branch intersects the main channel) and continuing to the branch end point.

Counts were done by month. Eventually, each month would yield four three-dimensional histograms. The first dimension was horizontal branch distance, sorted into 1 km bins. The second dimension was the predictor. Two histograms used altitude (one for the flash source point and one for the branch end point) in 300 m increments, and the other two used temperature (again, of the flash source and branch end) in 2°C increments. The third dimension was the azimuth of each branch from the flash source point in 10° bins. These monthly files were used as building blocks to allow analysis by year, season, or the entire data period.

3.3 Statistical Methods

Analysis of branch distance was done by percentiles in order to find meaningful information about the data distributions. A cumulative distribution function was used to determine the 50th, 90th, 95th, and 99th percentile distances. This was done in the vertical by collapsing the azimuthal information to a 2-D plane. In this case, percentiles were not based on azimuth, but rather solely upon vertical level. Likewise, for the azimuthal analysis, a single horizontal plane was examined, either by collapsing the array totals to one level or by looking at a specific vertical bin.

3.4 Sources of Error

3.4.1 LDAR Error. The first source of error in the study comes from the LDAR data itself. The sources of LDAR error were described in some detail in Section 2.4. LDAR has a location error that increases logarithmically as distance increases from Site 0. Less tangible is the error stemming from the 110 μs blackout time between listening periods, which can miss parts of the lightning process.

3.4.2 Flash-Grouping Error. The flash grouping algorithm attempted to apply scientific reasoning to the LDAR data, using what is known about the lightning process to build flashes from signals that should be lightning and to filter out those that are probably not. The algorithm was not foolproof, however, and there was no real way to know for certain that a group of signals, which meet the algorithm's criteria for a lightning flash or branch, really is such. Samples were examined by hand and plotted, and tended to follow a conceptual model of lightning in terms of horizontal and vertical extent, orientation, and branching. The assumption must then be made that the majority of the grouped flashes are indeed lightning with the knowledge that they may not all be.

3.4.3 Branch Distance Error. Distances were calculated from the flash source to each point in each branch, and the farthest point in each branch became the branch end point. This was a horizontal distance, so it did not account for vertical changes in the channel, and so did not reflect the true channel length. The aforementioned LDAR blackout period could have caused some additional points at the end of a branch to be missed, so in some cases, branches may have been longer than the data indicated.

3.4.4 Sounding Error. Sounding data came from a different location than much of the lightning data. The Cape Canaveral rawinsonde launch site is located at 28.48° N, 80.55° W, which puts it roughly 11.1 km from LDAR Site 0. Since flashes originating within 60 km of LDAR Site 0 were examined, the distance from the sounding site to flash source point can be as much as 71.1 km. In fact, since branches propagating past 60 km from LDAR Site 0 were included (the 60 km restriction applied only to the first point in a flash), the distance between LDAR points and the sounding could have been even farther. The magnitude of the error could vary widely from a very small value (perhaps less than

1°C) under a stagnant tropical airmass to large differences (several °C) in the occasional event of a synoptic boundary between the lightning data and the balloon path. This error would also vary by season and altitude. Balloons can also drift several kilometers during their ascent, in some cases away from the LDAR data sources. All of these factors could have contributed to errors in the results. The temperature and altitude data from these balloons is subject to minor instrumentation error as well.

3.4.5 Temperature Error. An interpolation scheme was used to take the temperature data from mandatory and significant sounding levels to create an array of temperatures at even intervals. The scheme was linear in altitude, so it assumed a straight-line temperature trace between the inflection points represented at the mandatory and significant levels. The real profile may not have been linear in every case, so therein was a source of error. Each column in the temperature array described in Section 3.2.2 represented a different sounding, either from the previous day, the day in question, or the following day. If a sounding were cut off below 25.5 km, the next nearest-neighbor sounding was used to complete the array above the cut-off altitude. This was another source of interpolation error, including that created when a daytime and nighttime sounding may have been mixed. There was also a timing error, since data points often lay several hours away from a sounding time. Temperatures at altitude did change between sounding times.

Table 2 shows the error between soundings at mandatory levels. Mean Absolute Error (MAE) was calculated first, and illustrates the average change in temperature between consecutive soundings. The MAE was less than the chosen 2°C error limit for this study for all mandatory levels but 500 mb, which showed a greater change than the

others. Root Mean Square Error (RMSE) was also calculated for statistical comparison, and is greater than the MAE for all levels. These statistics were calculated following Wilks (1995). However, a lightning flash could have occurred at most halfway between sounding times, so the real error associated with assigning a temperature to a flash is more likely to be half or less of the quantities shown, assuming a constant (linear in time) temperature change between soundings. Another consideration affecting these errors is that mandatory levels did not remain at the same altitudes, and in some cases varied in altitude between sounding times by enough to fall into different 0.3 km altitude bins. Also, the number of soundings reporting the mandatory levels in Table 2 decreased from 3512 soundings reporting 1000 mb to 3476 soundings reporting 300 mb.

Table 2. Temperature Error by Mandatory Level. Temperature error between successive soundings is shown from 0000 UTC 1 March 1997 through 2200 UTC 31 May 2001.

Temperature Error by Mandatory Level						
Statistic	1000 mb	850 mb	700 mb	500 mb	300 mb	200 mb
Mean Absolute Error (MAE) (°C)	1.44660	0.89553	0.79192	2.32251	1.31895	0.97410
Root Mean Square Error (RMSE) (°C)	3.43491	1.54024	1.37420	4.19313	2.81287	1.83248

3.4.6 Sampling Error. There was little that could be done to take into account the degree to which the vertical temperature profile was disturbed by convection, and it is nearly impossible to tell for sure what the temperature distribution was within a thunderstorm. Indeed, it is almost guaranteed that the temperature profile within the thunderstorms differed from the synoptic sounding to some non-quantifiable degree. However, in the absence of temperature data from within the active storms, and in the assumption that updraft and downdraft temperature distortions should average out over time, this error should not invalidate the work completely, but should be considered as a limiting factor.

3.4.7 Counting Error. A final source of error came from the counting scheme. Distances were truncated to their whole kilometer values for the purposes of placing them in histogram bins. The same was done in the vertical (300 m bins and 2°C bins) and by azimuth (10° bins). The 1 km distance bin width was considered adequate, since the USAF uses a distance to the whole nautical mile for lightning avoidance. The 300 m and 2°C vertical bin widths correspond, as mentioned in Section 3.2.2, to roughly 1000 ft altitude increments. The 10° azimuth bins were considered adequate, because they match the degree of precision for upper-level wind forecasts and observations.

IV. Results and Analysis

4.1 Maximum Horizontal Branch Distances

Initial investigation of the maximum horizontal branch distances yielded surprising results. Before the data were reduced to only those branches whose flash source was within 60 km of LDAR, many of the maximum distances were well over 160 km. These values were mostly likely the result of gross error since they occurred at the extremes of the LDAR sensing range (several hundreds of kilometers). The distance error in the flash grouping algorithm at this range from LDAR is so large that the algorithm becomes unreliable.

The maximum branch distances for those flashes originating within 60 km of LDAR for the period 1 Mar 97 through 31 May 01 are displayed in Figure 6. Here the maximums still exceeded 100 km at many levels. While there is no scientific reason to discount the possibility of lightning traveling that distance, there is a good probability that LDAR location error and the limitations of the flash-grouping algorithm affected the distance values. A feature of note in these plots is that distances were longer at higher altitudes based on the vertical level of the branch end point than that of the flash source point. It could be that some of the longer flashes were propagating upward as well as laterally. In fact, some of the branch end points at higher altitudes had to have originated as much as 10 km lower. This is indicated by the appearance of the same maximum distance in both plots at different altitudes in Figure 6. Further study tended to support the supposition of vertical propagation. Unfortunately, maximum values can be

misleading since it is difficult to distinguish from single data points whether the information is real or a function of error.

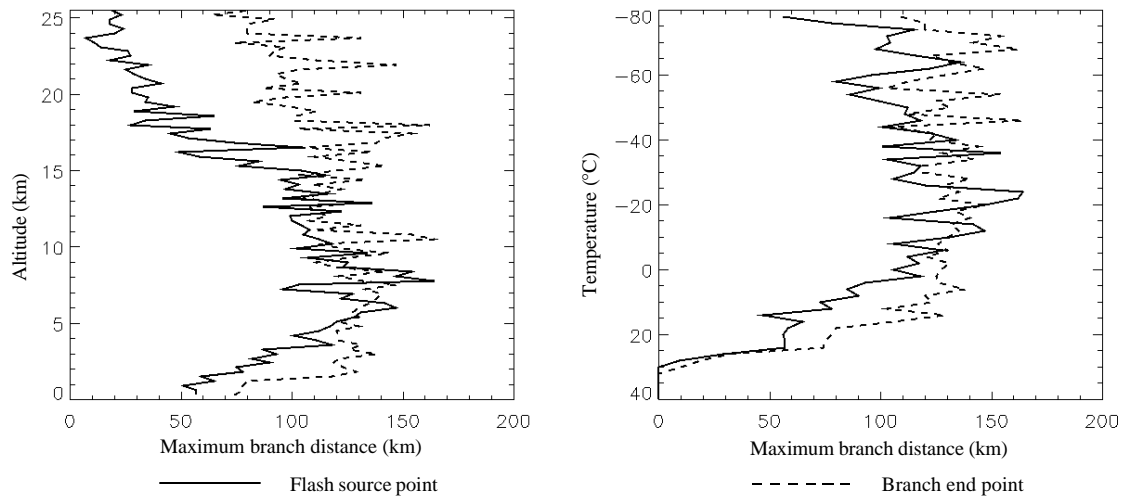


Figure 6. Maximum Horizontal Branch Distances by Altitude and Temperature. Distances are displayed first as a function of flash source (solid) and branch end point (dashed) altitude, and by flash source (solid) and branch end point (dashed) temperature.

4.2 Statistical Distribution of Branch Distances

The branch counts were distributed by horizontal distance and vertical level (Figure 7), summing over all of the azimuths. The horizontal branch distances were plotted by the flash source and branch end altitudes, and by flash source and branch end temperatures. All four plots showed a very pronounced peak in branch counts at less than 5 km horizontal distance, with branch counts dropping off rapidly with increasing distance. The flash source altitude plot (Figure 7a) showed a double peak in branch counts, with the larger peak near 9 km altitude and the smaller near 6 km altitude. A single peak near 7 km altitude (Figure 7b) appeared in the branch end point plot. Another double peak was apparent in the flash source temperature data (Figure 7c), with the larger peak near -28°C and the smaller near 4°C . Lastly, the branch end point temperature distribution (Figure 7d) showed the most complex structure with several peaks, the

largest being near -12°C . The double peaks in the flash source plots may correspond to the upper positive (larger peak) and main negative (smaller peak) charge centers in the dipole thunderstorm model. The less pronounced peaks in the branch end point temperature data may then suggest that some flashes had a vertical component to their propagation; purely horizontal channels should have resulted in identical branch count distributions between flash source and branch end points.

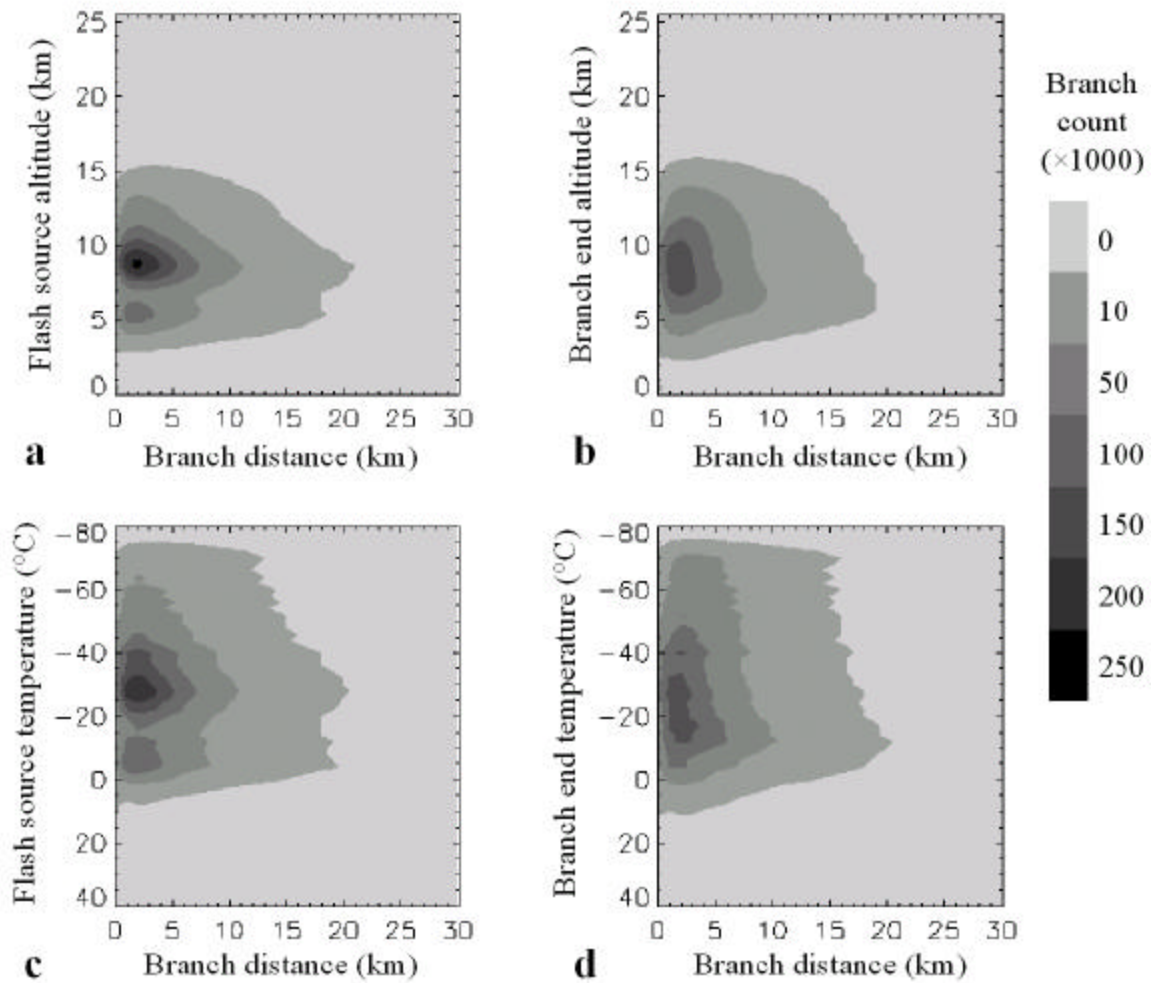


Figure 7. Distributions of Branch Counts. Counts (thousands) are plotted by horizontal distance (x axis) and vertical level (y axis). Vertical levels are flash source altitude (a), branch end altitude (b), flash source temperature (c), and branch end temperature (d). Contour interval is indicated at right.

The maximum branch count was found at 7.2 km altitude and at -12°C for branch end point data. The branch end point altitude is of prime concern to aviators, and the branch end point temperature is both a more accurate estimation (since it is often outside of the thunderstorm and similar to the environmental conditions measured by rawinsonde) and should be closer in value to the outside air temperature (OAT) measured by an aircraft.

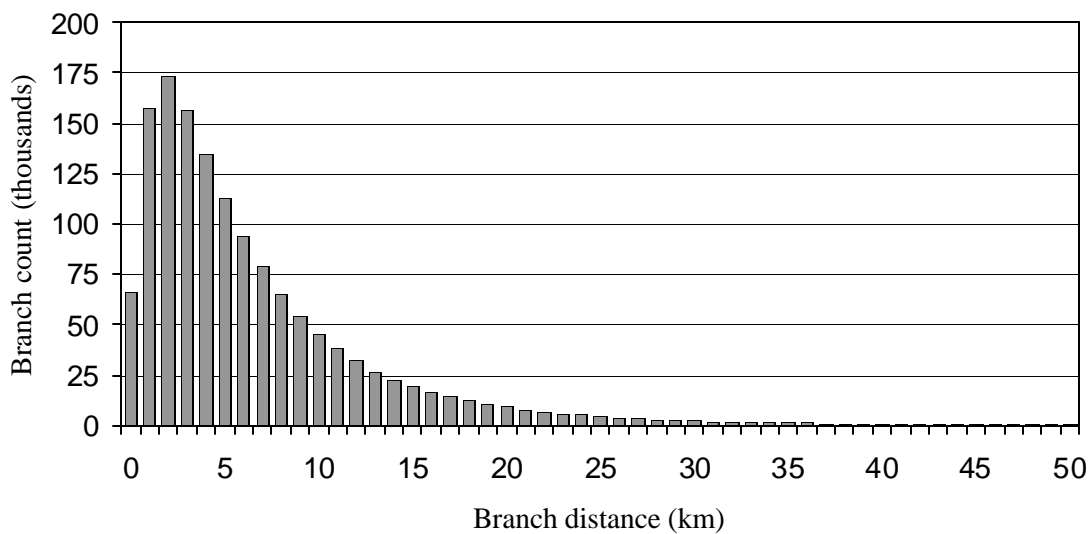


Figure 8. Frequency Distribution of Horizontal Branch Distances for Branches Ending at 7.2 to 7.5 km Altitude.

For branches ending between 7.2 and 7.5 km altitude (Figure 8), the data appeared to have a gamma distribution. The mode of the branch distances was 2 km (173,539 branches), and the median branch distance was 5 km. The maximum branch distance was 113 km, but the branch count in that bin was only 1. For branches ending in the -12°C bin, the mode of the distance was also 2 km (with a branch count of 160,799), and the median branch distance was also 5 km. The maximum branch distance was 135 km with

a bin count of 1. In fact, beyond 50 km distance in both cases, branch counts remained in the single digits, often separated by zeroes.

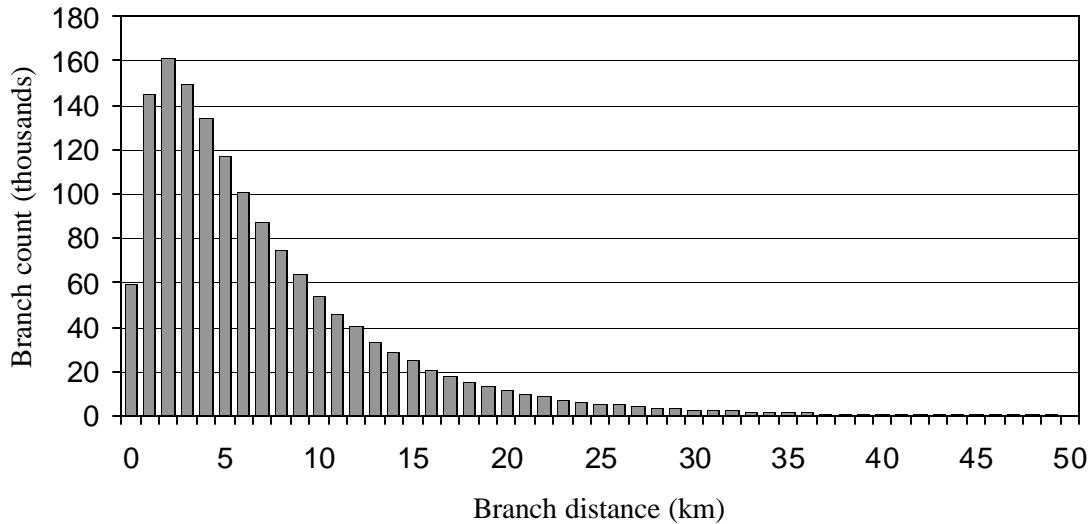


Figure 9. Frequency Distribution of Horizontal Branch Distances for Branches Ending at -10° to -12°C .

One of the dangers of simply examining the maximum branch distance at each vertical level is that the number of data points, or sample size, for that distance bin may be small. For example, the maximum branch distance by branch end point was 164 km at 10.5 km altitude. There was only 1 branch in that bin. The next longest branch was 108 km long, also a single-branch bin. In fact, 53 km was the longest branch distance ending at that altitude with more than 100 branches in the bin.

As will be seen in the 99th percentile of branch distance plots in Section 4.3, the higher vertical levels show considerable variation in branch distance, as do the higher temperatures (which correspond to levels near the surface). The postulation is that the sample sizes at these levels were too small to accurately reflect the population of branches. To test this hypothesis, histograms were built for vertical levels at which variation in distance was more pronounced. The levels chosen to represent the smaller

sample sizes were the 25.2 km branch end altitude bin and the 26°C branch end temperature bin, and are shown in Figures 10 and 11, respectively.

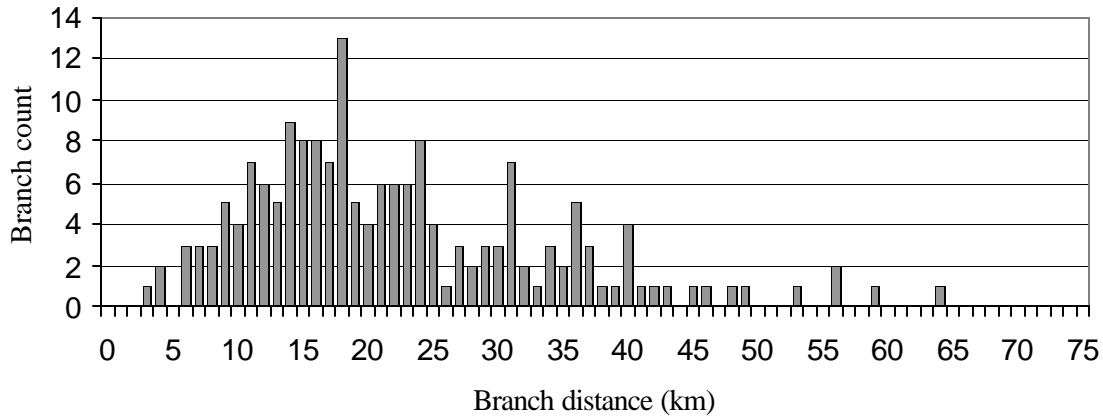


Figure 10. Frequency Distribution of Horizontal Branch Distances for Branches Ending at 25.2 to 25.5 km Altitude.

The most striking feature in Figure 10 is the deviation from the gamma distribution of the branch counts. The mode was 18 km (13 branches) and the median was 19 km, though branch counts in this distribution were five orders of magnitude smaller than 7.2 km altitude. The maximum branch distance was 64 km, but only 1 branch held that bin. The frequency distribution at 26°C (Figure 11) showed a marked preference for short branches, with the mode and median values being 0 km (all branches less than 1 km in length). At 0 km distance, there were 1178 branches, as compared to the maximum horizontal distance of 32 km, which was attained by only one branch. The most likely explanation for this distribution is that the 26°C level was most often near the surface, so the vast majority of lightning flashes through this layer were CG, and therefore primarily vertical. Most of the branches from these flashes were also likely to have a strong vertical component.

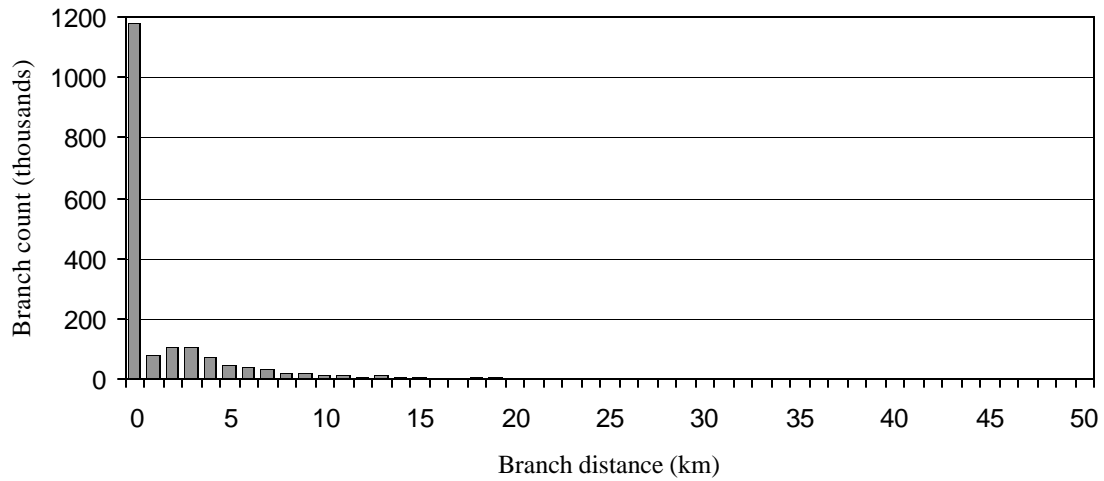


Figure 11. Frequency Distribution of Horizontal Branch Distances for Branches Ending at 28° to 26°C.

4.3 Percentiles of Branch Distance – Total Period

As previously demonstrated, maximum horizontal distance values were not necessarily representative of the true distributions of the data. Therefore, percentiles of distances were examined. Figure 12 depicts the vertical distribution of specific percentiles of horizontal branch distance, using the values of altitude and temperature of the branch end points as the vertical coordinate. The percentiles of distance were determined as in Section 3.3, and are given in tabular format in Appendices A and B. At first glance, median (50th percentile) values were much shorter than the maximum, being typically about 5 km in length. The 90th percentile of branch distance over the entire data period was as much as 100 km short of the maximum at many levels. The 95th percentile of distance was less than 10 km longer than the 90th percentile. The 99th percentile was chosen for further study because the distances were closer to the maximum and so were of more use to aviators in attempting to avoid lightning, but was not contaminated by the

extreme values. Indeed, extreme values are difficult to quantify. They are infrequent and do not necessarily represent an absolute ceiling.

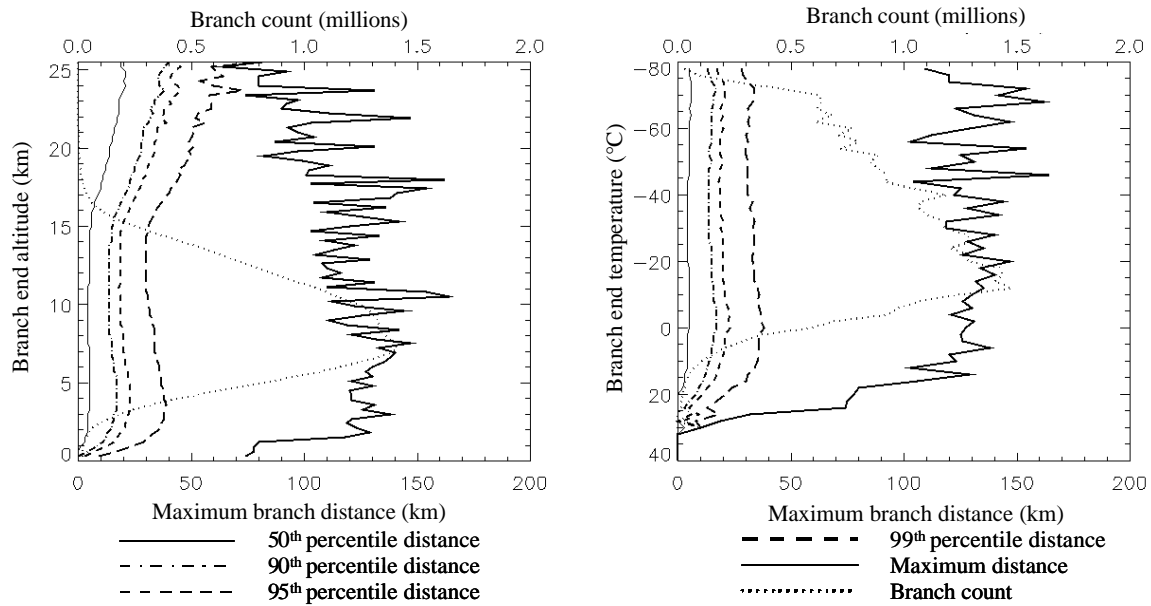


Figure 12. Percentiles of Branch Distance Based on Altitude and Temperature of the Branch End Points.

In all cases, branch counts were included to indicate the sample size, and therefore provide information about the reliability of the results. Since the data were not normally distributed, branch count was one of the few ways to quantify reliability. The assumption was that the larger the sample size, the more reliable the results.

4.3.1 99th Percentile (Total Period) – Vertical Distributions. Data from the entire period of 1 Mar 97 through 31 May 01 were examined first. The 99th percentile of branch distance was plotted by altitude of the flash source points and of the branch end points (Figure 13). The maximum 99th percentile of the distance by flash source altitude was 41 km at 2.7 km altitude. The maximum 99th percentile of the distance by branch end point altitude was 81 km at 25.5 km altitude, though the branch count here was only 28. Since 25.5 km is so much higher than the tropopause, data from that level, as well as

anything above 17 km, is suspect. Branches originating above 17 km altitude accounted for only 0.15% of the data from the period of record. While transient luminous events (TLEs) such as sprites and blue jets may have occurred at these levels, it is doubtful that they were the sole explanation. LDAR vertical location errors and anomalous signal detection at high altitudes were probably to blame for some of these results.

More interesting were the values below 17 km altitude. The longest 99th percentile distance values by flash source altitude were 35 to 41 km in the 2 to 7 km altitude range, while by branch end altitude the longest were 34 to 39 km in the same altitude range. Equally interesting were the branch counts. The maximum branch count by flash source altitude was 2,027,797 at 8.7 km. There was a secondary maximum of 1,038,259 branches at 5.7 km altitude. The maximum branch count by branch end point was at 7.2 km altitude, with a value of 1,408,138.

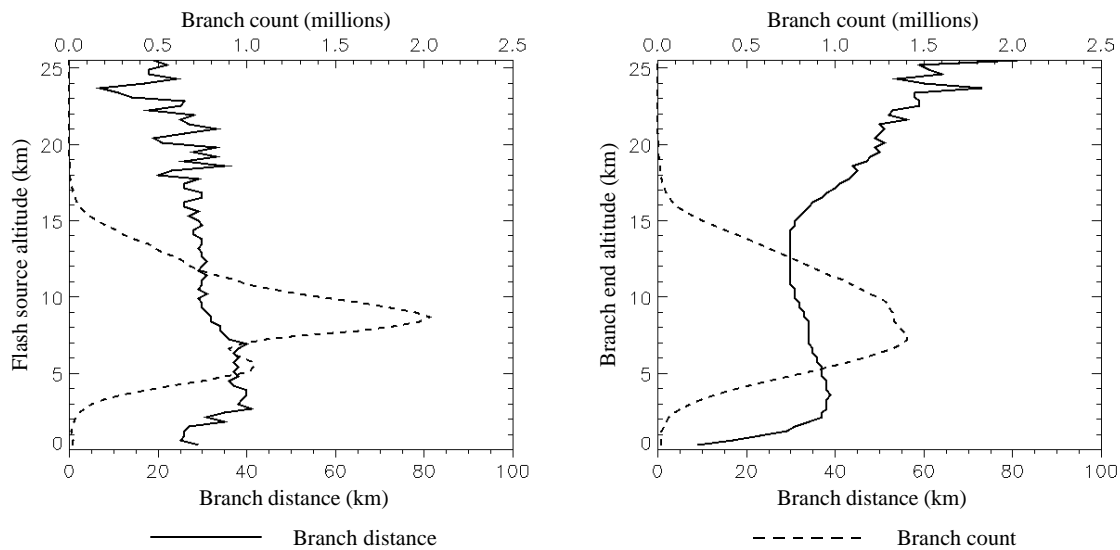


Figure 13. 99th Percentile of Branch Distance by Altitude (Total Period). Distances were plotted by flash source altitude and branch end point altitude. 99th percentile of branch distance is solid; total branch counts are dashed.

The distribution of branches ending in the 3 km altitude bin (representing the region of longest 99th percentile distance values) shown in Figure 14 displayed a similar distribution to that in Figure 8. The mode for this distribution was 2 km, and the median distance was 5 km. The maximum distance was 138 km, though again, only one branch held that bin. The high branch counts at 3 km altitude and the similar gamma distribution lent credibility to the results.

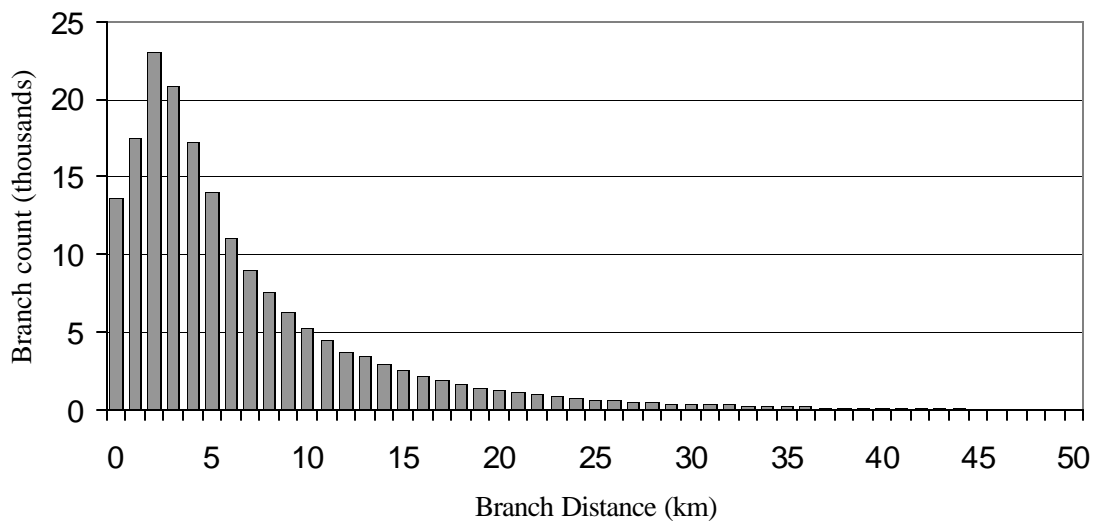


Figure 14. Frequency Distribution of Horizontal Branch Distances for Branches Ending at 3 to 3.3 km Altitude.

The 99th percentile of flash distance was then compared to flash source point temperature and branch end point temperature (Figure 15). The maximum 99th percentile of distance by flash source temperature was 35 to 39 km between 8° and -20°C. The maximum 99th percentile of flash distance by branch end point temperature was 35 to 38 km between 10° and -12°C. The maximum branch count by flash source temperature was 1,940,397 at -28°C, with a secondary maximum branch count of 1,178,646 at -4°C. The maximum branch count by branch end point altitude was 1,477,860 at -12°C.

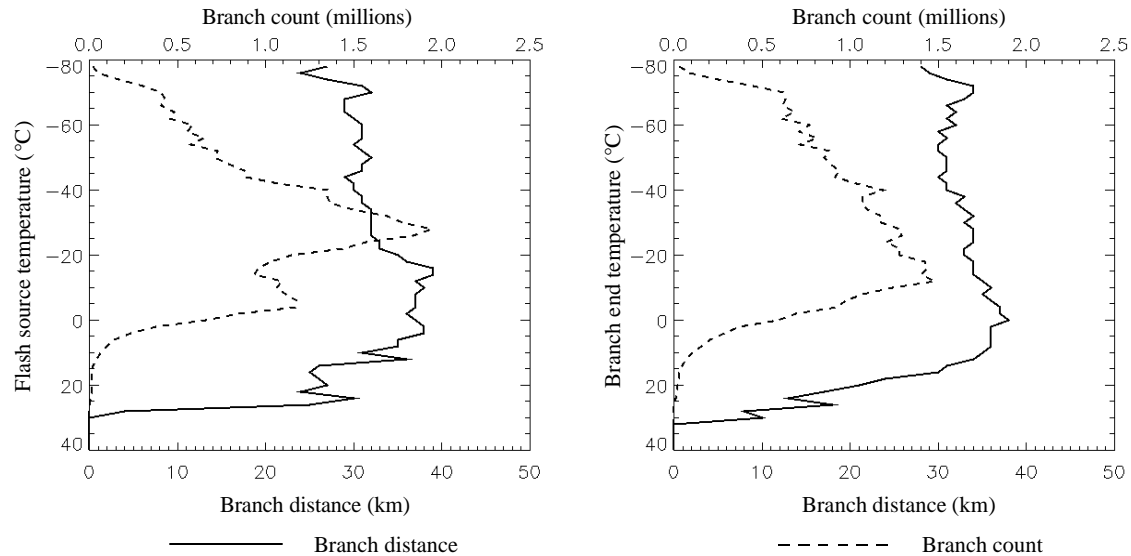


Figure 15. 99th Percentile of Branch Distance by Temperature (Total Period). Distances were plotted by flash source temperature and branch end point temperature. 99th percentile of branch distance is solid; total branch counts are dashed.

The maximum 99th percentile of distance by end branch point temperature was 38 km around 0°C. At this temperature, the distribution (Figure 16) is nearly identical to that of Figure 9. The mode here was still 2 km, and the median was 5 km. The maximum distance was 127 km, held by one branch.

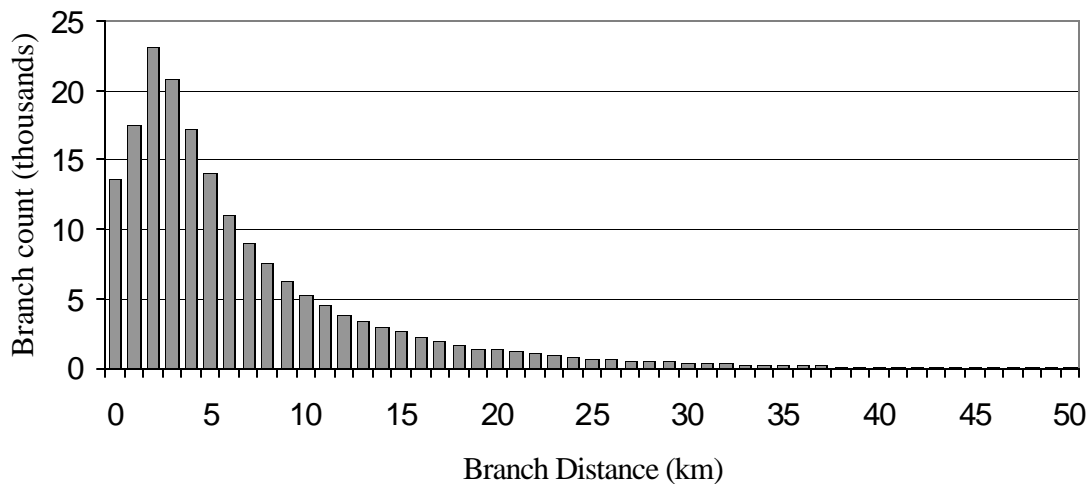


Figure 16. Frequency Distribution of Horizontal Branch Distances for Branches Ending at 2° to 0°C.

4.3.2 99th Percentile (Total Period) – Horizontal Distributions. The azimuth was determined as the compass direction from the flash source point to the branch end point. The vertical bins were then summed, and the 99th percentile of the distance of these sums was plotted by azimuth, shown in Figure 17. The slice at 7.2 to 7.5 km altitude was taken to correspond to the maximum branch count by branch end altitude in Figure 13. Here the distances were not integrated; only those branches in the 7.2 km altitude bin were considered.

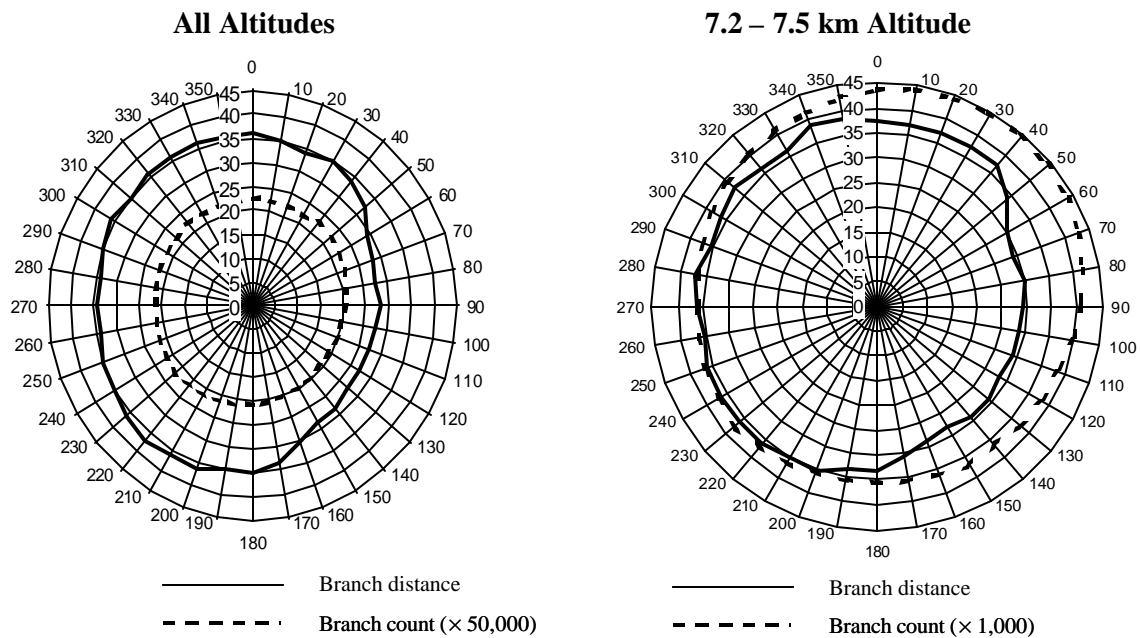


Figure 17. 99th Percentile of Distances and Total Branch Counts by Azimuth.

Shorter distance values were found to the east and to the southeast both in the case of the total data and at the 7.2 to 7.5 km altitude bin. Branch counts were slightly higher toward the northeast. These data were influenced by thunderstorm orientation and motion, the details of which are described by season in Section 4.8.

4.3.3 99th Percentile (Total Period) – Conclusions. The results were assumed to be more reliable where the branch counts were higher. Therefore, low branch counts at

higher altitudes and lower temperatures probably skewed the 99th percentile of distance above 15 km or -70°C (Figures 13 and 15). Since a relatively small number of branches were found at those levels, it is unlikely that their 99th percentile values were representative of the population over time. Similarly, the most reliable results were found in the 2 to 17 km and 10° to -70°C ranges. Longer channels were found between 2 and 7 km altitude in both altitude cases. The branch count maxima in the flash source altitude and temperature plot may correspond to thunderstorm charge regions as in Section 2.1, with the main negative region between 5 and 7 km (0° and -15°C) and the upper positive region roughly 7 to 12 km (-25° to -40°C). Also, the 99th percentile of distance was shorter when evaluated by branch end point altitude and temperature than by flash source altitude and temperature. However, this difference in horizontal difference is of the same order of magnitude as the LDAR location error.

4.4 99th Percentile of Distance - Spring

Seasonal variations were examined next. The spring values were taken from the months of March, April, and May for 1997-2001, with close to 10 million branches.

4.4.1 99th Percentile (Spring) – Vertical Distributions. For the spring season (Figure 18), the maximum branch count occurred at a slightly lower altitude than the total; 566,008 branches came from flashes originating at 8.1 km. For the branch end point altitude, the maximum branch count was 342,746 at 6.6 km altitude. A second peak of 340,078 branches occurred at 9 km branch end altitude. Below 17 km altitude, the longest 99th percentile distances by flash source were 40 to 45 km, occurring between 2 and 7 km altitude. Branches with 99th percentile distances of 39 to 42 km were found to

end at 2 to 7 km altitude as well. As in the total period, the longest channels were found once again in the 2 to 7 km range. The extreme variability in 99th percentile distance aloft was likely a result of small sample size at altitudes above 15 km.

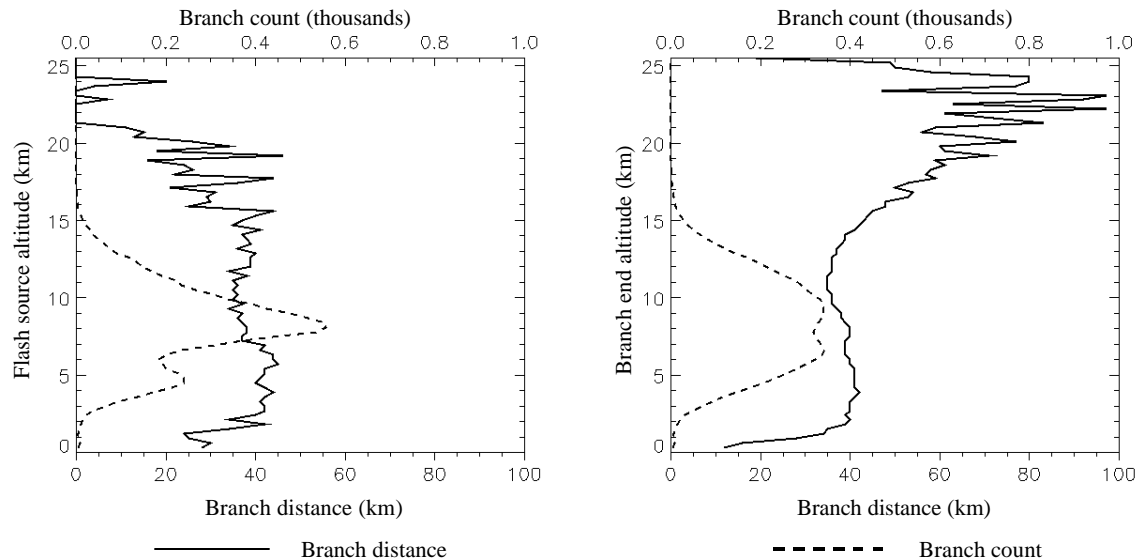


Figure 18. 99th Percentile of Branch Distance by Altitude (Spring). Distances were plotted by flash source altitude and branch end point altitude. 99th percentile of branch distance is solid; total branch counts are dashed.

Looking at spring 99th percentile of distance by temperature (Figure 19), it was clear that branch counts were well distributed from 10° to -70°C, giving credence to the results at these levels. Here the highest 99th percentile of horizontal branch distance by flash source temperature was 39 to 46 km, occurring at 4° to -22°C. The highest 99th percentile of distance by branch end temperature was 40 to 43 km, found between 10° and -14°C. An additional note of interest is that the temperature branch counts indicated that some branches might have had a vertical component, a phenomenon seen across most of the results. For example, the highest number of branches (517,866) originated at -38°C, but only 356,234 ended at that level. The flattened branch count distribution by

branch end temperature suggests that some branches propagated in the vertical as well as horizontal.

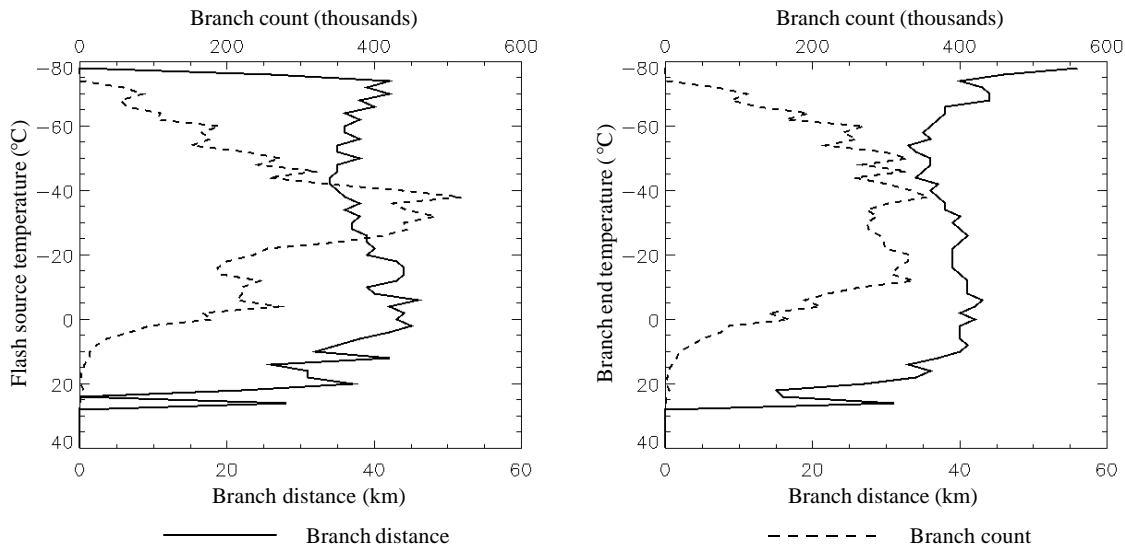


Figure 19. 99th Percentile of Branch Distance by Temperature (Spring). Distances were plotted by flash source temperature and branch end point temperature. 99th percentile of branch distance is solid; total branch counts are dashed.

4.4.2 99th Percentile (Spring) – Conclusions. The lower branch counts from 15 km and up tend to indicate that storm tops in the spring did not often exceed that altitude. The 2 to 7 km altitude region showed the longest 99th percentile of branch distance, as was the case for the total period. There were some indications of vertical as well as horizontal propagation in the branches. The similarity between the spring results and the total results indicated that the spring data had a significant influence on the total distribution.

4.5 99th Percentile of Distance - Summer

By far the most branches came from the summer months of June, July, and August of 1997-2000. Over 23 million branches were examined from this period.

4.5.1 99th Percentile (Summer) – Vertical Distributions. The summer distribution of 99th percentile of distance by altitude (Figure 20) shows the maximum branch count originating at 8.7 km altitude, as did the total period distribution (Figure 13). A total of 1,249,731 branches originated from flash source points at 8.7 km altitude. The maximum number of branches (875,752) ended at 7.5 km altitude. The 99th percentile distance values showed the longest branches again between 2 and 7 km altitude (34 to 40 km by flash source altitude and 32 to 36 km by branch end altitude). Shorter distances (28 to 31 km) were found between 7 and 13 km altitude. Results above 17 km altitude were suspect, as the branch counts were very low.

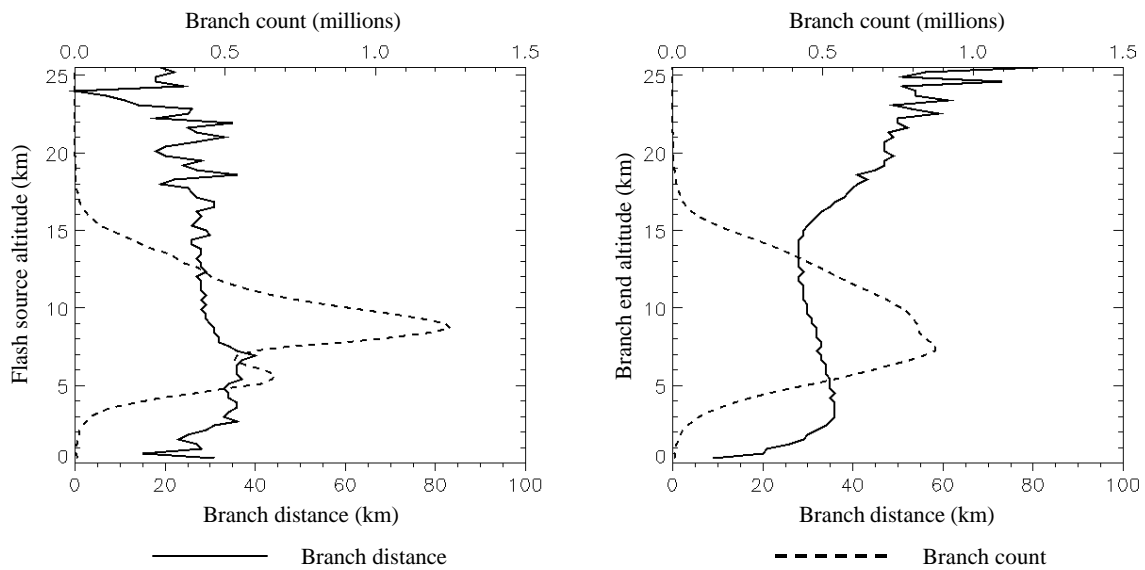


Figure 20. 99th Percentile of Branch Distance by Altitude (Summer). Distances were plotted by flash source altitude and branch end point altitude. 99th percentile of branch distance is solid; total branch counts are dashed.

Distributions by temperature in the summer months (Figure 21) showed a disparity between distances by flash source temperature and distances by branch end temperature. Flash source temperature showed a sharper distinction between longer branches at higher temperatures (lower levels) and shorter branches at lower temperatures

(higher levels). The 33 to 38 km branch distances were found from 10°C to -20°C, with the shorter 27 to 32 km distances found above that. This distinction was less pronounced with respect to branch end point temperature. Instead the 10° to -20°C distance values were 32 to 36 km, with 29 to 32 km distances above that. These differences in distances were greater in magnitude than the LDAR location error.

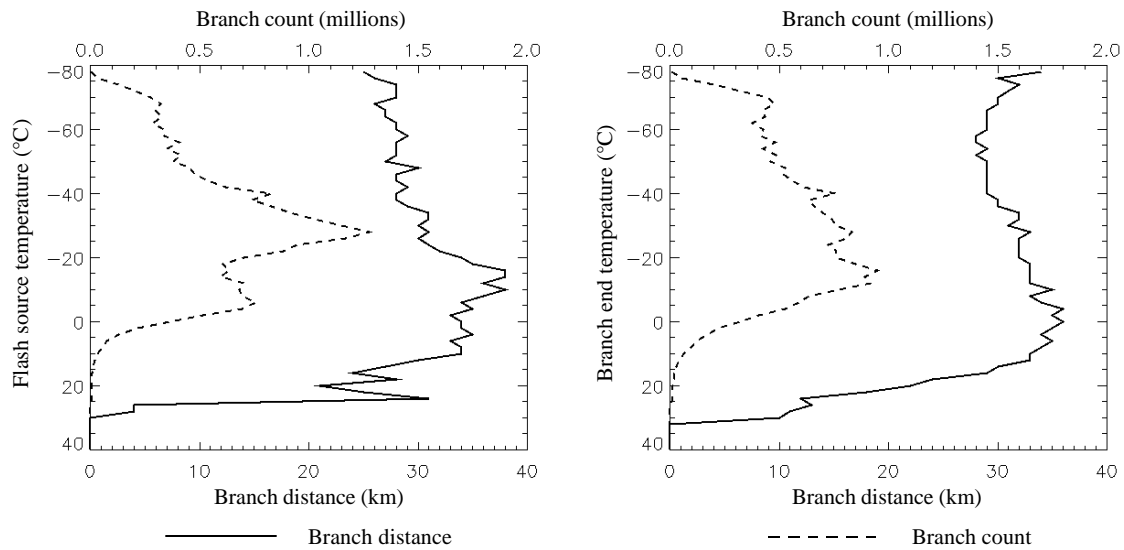


Figure 21. 99th Percentile of Branch Distance by Temperature (Summer). Distances were plotted by flash source temperature and branch end point temperature. 99th percentile of branch distance is solid; total branch counts are dashed.

4.5.2 99th Percentile (Summer) – Conclusions. Summer saw the most lightning activity, with roughly 59% of the total branches for the period (1 Mar 97 to 31 May 01) occurring in the months of June, July, and August. The summer months exerted the greatest influence over the total data set. Summer distributions of the 99th percentile of branch distance by altitude mirrored those of the total period. The longest branches were found at 2 to 7 km altitude, and originated between 10° and -20°C.

4.6 99th Percentile of Distance - Autumn

The autumn months of September, October, and November (1997-2000) were examined next. There were 5.5 million branches in this period. The 99th percentile of distance showed more variation in the vertical than for spring and summer.

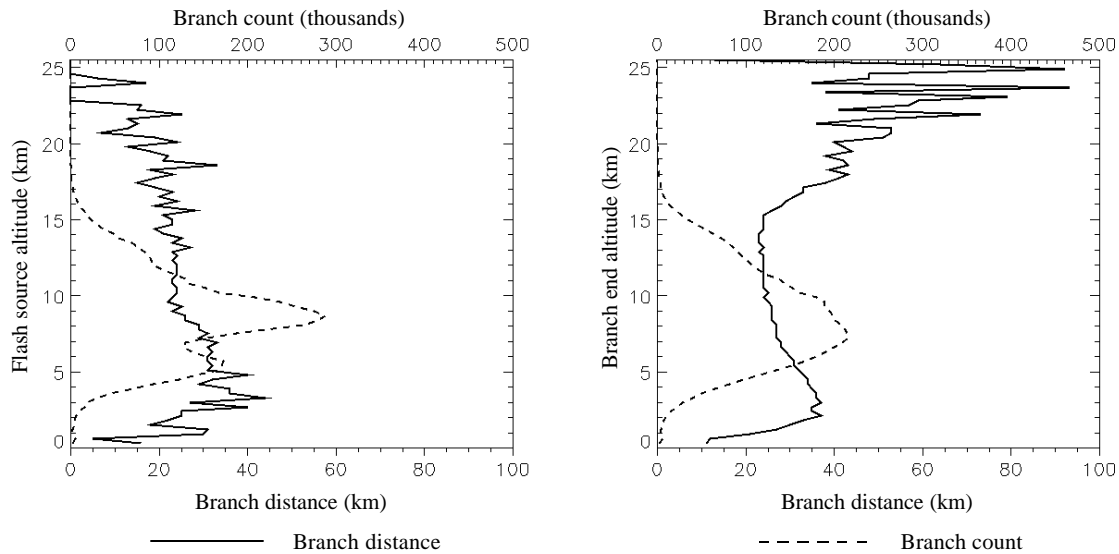


Figure 22. 99th Percentile of Branch Distance by Altitude (Autumn). Distances were plotted by flash source altitude and branch end point altitude. 99th percentile of branch distance is solid; total branch counts are dashed.

4.6.1 99th Percentile (Autumn) – Vertical Distributions. The distribution of 99th percentile of distance by flash source altitude (Figure 22) showed the peak of branch distances at the 2 to 9 km altitude level, though there was considerable variability in the distances. The 99th percentile of distance here ranged from 25 to 44 km. Above 9 km altitude, the 99th percentile distances dropped off to 19 to 24 km. The branch end point curve was smoother, with maximum values of 30 to 37 km in the 2 to 6 km altitude range. The maximum branch count by flash source altitude was 288,092 at 8.7 km with a secondary maximum of 172,245 branches at 5.7 km altitude. The maximum branch

count by branch end altitude was 215,040 at 7.2 km altitude. Here again, low branch counts above 17 km altitude led to erratic and presumably unreliable results.

The longest 99th percentile of branch distance values were found to originate at temperatures between 8° and -24°C (Figure 23). Those values ranged from 27 to 36 km, with shorter values at temperatures below -20° and above 16°C. The longest 99th percentile of branch distance by branch end temperature were 29 to 35 km, found from 12° to -16°C.

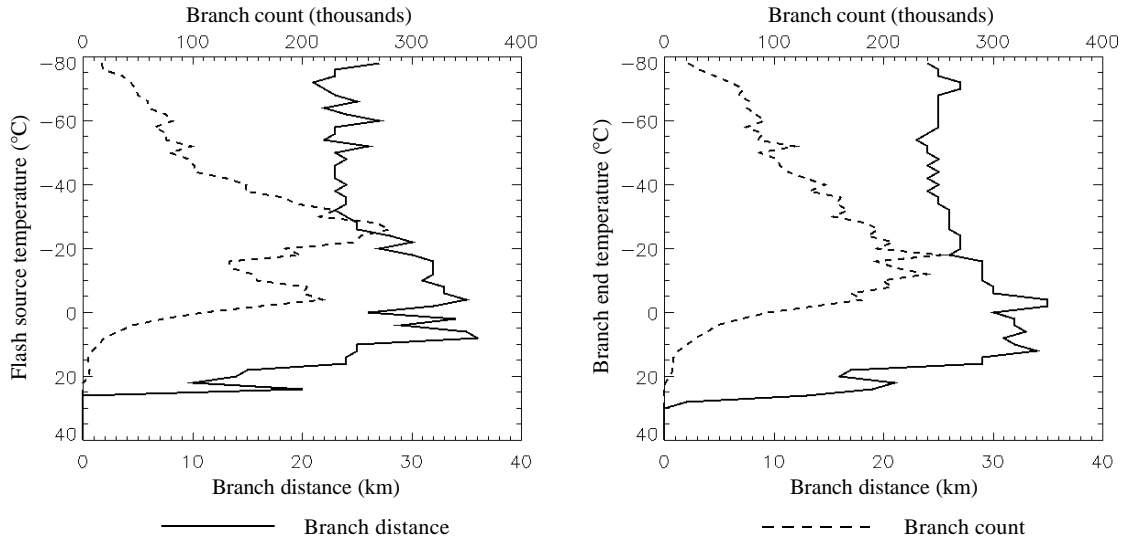


Figure 23. 99th Percentile of Branch Distance by Temperature (Autumn). Distances were plotted by flash source temperature and branch end point temperature. 99th percentile of branch distance is solid; total branch counts are dashed.

4.6.2 99th Percentile (Autumn) – Conclusions. The maximum branch counts were found between 7 and 9 km altitude, as were the counts from the total period. The longest branches were found in the 2 to 9 km altitude range, a slightly broader bracket than that encompassing the longest branches in the total period. The longest branches tended to occur at the same temperature levels in autumn as they did in summer and over the entire

period. The consistency is likely due to the relatively minor seasonal temperature changes over the KSC area between summer and early autumn.

4.7 99th Percentile of Distance - Winter

The winter months showed the least lightning activity. The months examined were December 1997-2000, January 1998-2001, and February 1998-2001. During this time period, slightly over 1 million branches were examined, representing less than 3% of the branch count for the total period.

4.7.1 99th Percentile (Winter) – Vertical Distributions. As would be expected, the lower thunderstorm tops of the winter season were reflected in the lightning data (Figure 24). The most branches (92,069) originated at 7.5 km, a full 1.2 km lower than that for summer and the total period. At each level, all of the branch counts were less than 100,000, and the variability from the relatively lower counts was evident in the 99th percentile of branch distances. Another interesting feature of the winter distribution was evident in the highest branches. Despite the fact that the flash source altitude data cut off at 17 km, the presence of data up to 24 km for branch end altitude indicated that at least some branches propagated upward by as much as 7 km in the vertical, though branch counts at these levels were in the single digits.

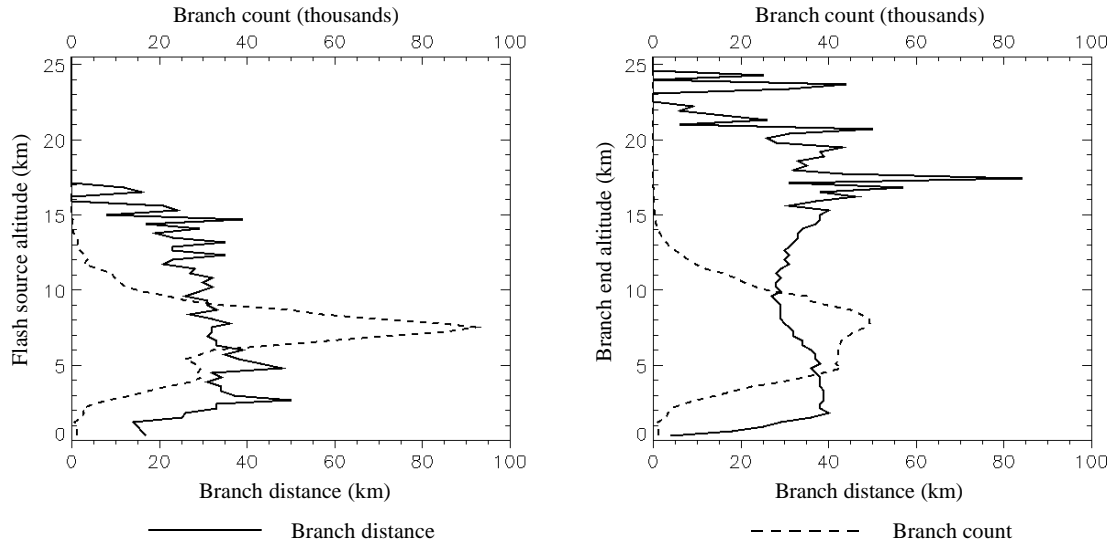


Figure 24. 99th Percentile of Branch Distance by Altitude (Winter). Distances were plotted by flash source altitude and branch end point altitude. 99th percentile of branch distance is solid; total branch counts are dashed.

The temperature distribution (Figure 25) also showed the difference in branch counts between flash source point and branch end point. The highest number of branches (103,963) started at -22°C , but only 62,074 branches ended there. Since the branch counts by branch end temperature were higher above -22°C than they were by flash source temperature, most of the remaining branches probably had an upward component. The 99th percentile of distance by flash source temperature was highly variable, ranging from 26 to 50 km from 10° to -40°C . The longest 99th percentile of distance by branch end temperature ranged between 27 and 42 km in the 16° to -40°C range.

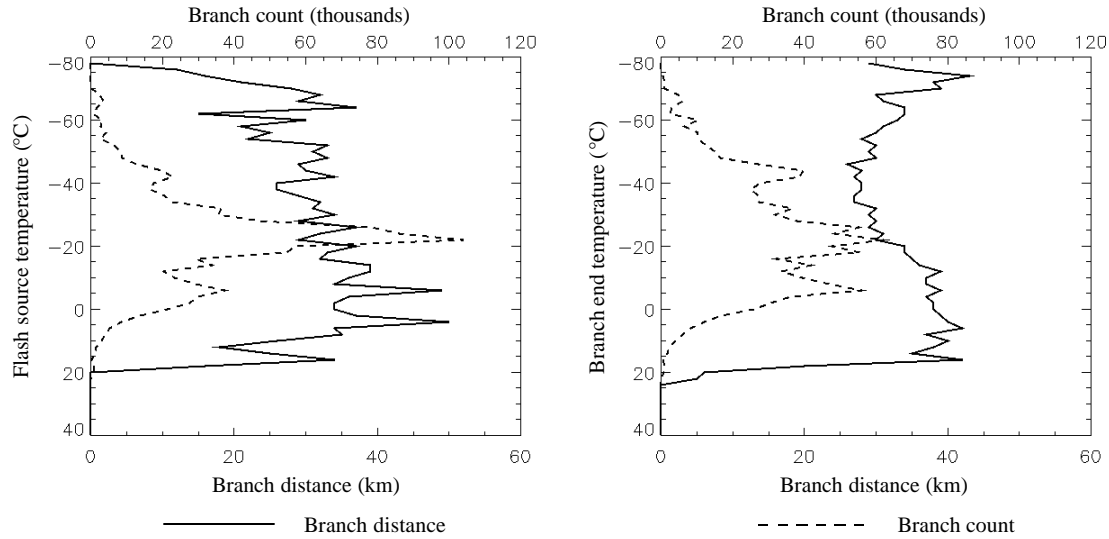


Figure 25. 99th Percentile of Branch Distance by Temperature (Winter). Distances were plotted by flash source temperature and branch end point temperature. 99th percentile of branch distance is solid; total branch counts are dashed.

4.7.2 99th Percentile (Winter) – Conclusions. Winter showed a number of branches with a vertical component, though the majority seemed to remain mostly horizontal as evidenced by actual branch count. Possibly the lower thunderstorm tops in winter made this phenomenon more obvious, or perhaps there was in fact an increase in winter of upward-propagating lightning. Indeed, temperature plots from all seasons show some degree of upward propagation via the branch counts, especially the springtime data, but winter data reflects this in the altitude plots more clearly than in the other seasons. Additionally, the winter data seems to reflect a specifically upward component. The longest branches were found between 16° and -40°C.

4.8 Summary of Vertical Distributions

The vertical distributions from the total period and the seasons all showed maximum 99th percentile of distance values near or overlapping the 2-7 km altitude and 10° to -20°C ranges. Table 3 compares the range of 99th percentile of distance values

within these ranges by season and for the total period of record. In most cases, the differences by season can be considered significant in that they are greater in magnitude than the LDAR location error. Winter showed the longest 99th percentile of horizontal branch distance, but also showed the greatest variability.

Table 3. 99th Percentile of Distance by Predictor and Season. Values are the range of 99th percentile of distance for the 2 to 7 km altitude range and the 10° to -20°C temperature range.

99 th Percentile of Distance by Predictor and Season					
Predictor	Spring	Summer	Autumn	Winter	Total
Flash Source Altitude (2-7 km)	40-45 km	27-40 km	25-44 km	31-50 km	35-41 km
Branch End Altitude (2-7 km)	39-42 km	32-36 km	28-37 km	32-39 km	34-39 km
Flash Source Temperature (10° to -20°C)	39-46 km	33-38 km	25-36 km	31-50 km	35-39 km
Branch End Temperature (10° to -20°C)	39-43 km	32-36 km	26-35 km	34-42 km	35-38 km

4.9 99th Percentile (Seasonal) – Horizontal Distributions

The 99th percentiles of vertically integrated branch distances were investigated by season. Since the vertical component was collapsed into a 2-dimensional plane, flash source and branch end altitude and temperature information was suppressed to instead examine simply the 99th percentile of horizontal distance versus the azimuth from flash source to branch end point.

Horizontal distributions by azimuth for spring (Figure 26) showed a slight elongation toward the northeast and southwest. The branch counts also increased in these directions. This may be due to the occasional synoptic-scale boundary oriented southwest to northeast moving through in early spring, with cloud flashes between cells in the line. The maximum 99th percentile of distance for spring was 46 km at 220°, with a secondary maximum at due north of 40 km. The shortest 99th percentile of distance was 32 km to the east and southeast. The maximum branch count of 309,153 was found at 40°, with a minimum of 247,724 branches found at 130°.

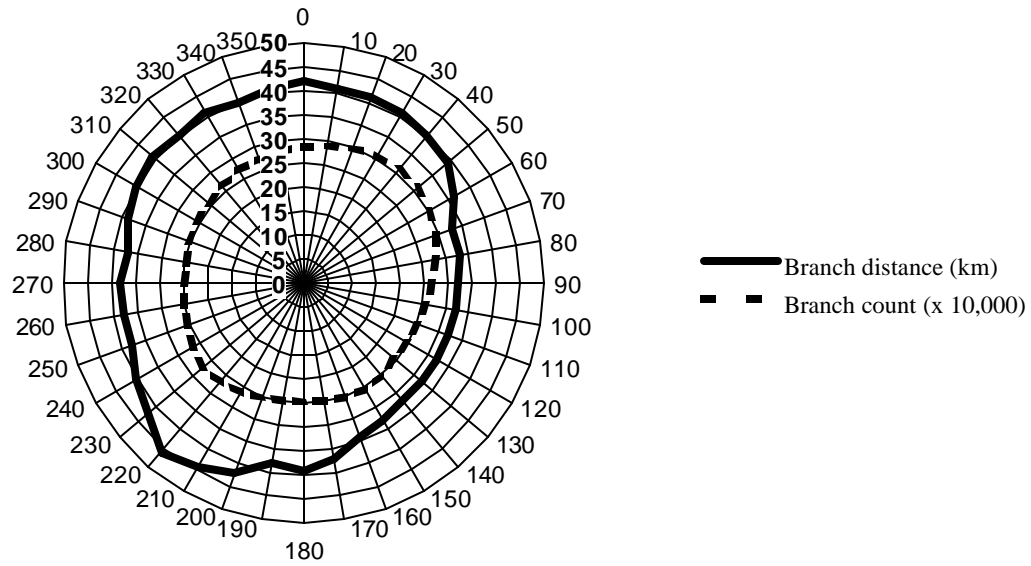


Figure 26. 99th Percentile of Branch Distance by Azimuth for Spring.

The summer azimuth plot (Figure 27) showed shorter 99th percentile distance values than spring. Here the elongation was more toward the south, and shorter distances were found to the east. The longest of the 99th percentile of distance was found to be 35 km, occurring at 180° and 240°. The shortest was 25 km toward the southeast. The maximum number of branches was 709,370 at 290°. The fewest branches (561,306) traveled toward 130°. A possible reason for the behavior of the 99th percentile of branch distance is the north-to-south orientation of sea breeze-frontal thunderstorms along the east coast of Florida in the summer, with cloud-to cloud flashes propagating between and through the cells.

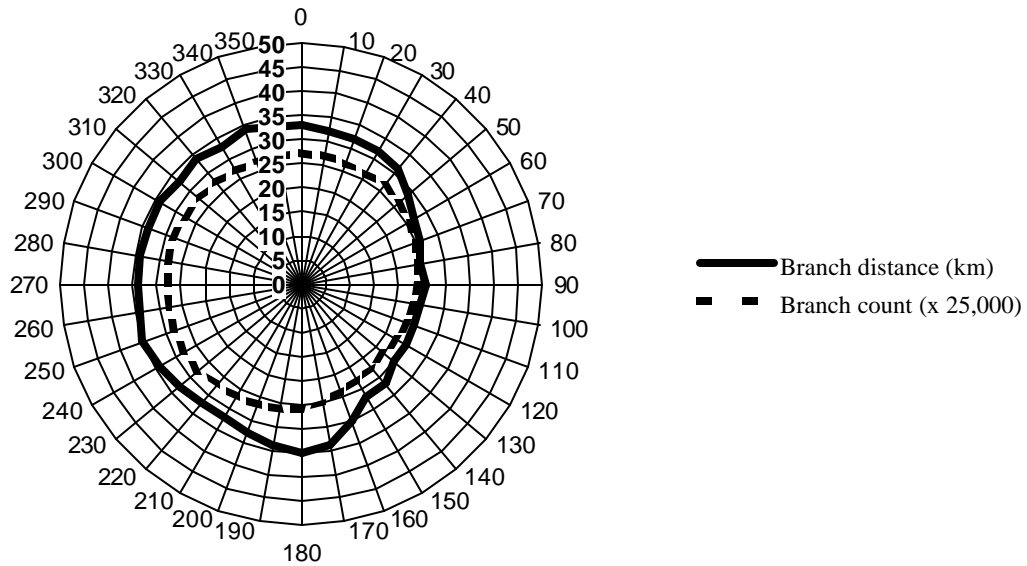


Figure 27. 99th Percentile of Branch Distance by Azimuth for Summer.

In the fall (Figure 28), there was still a shortening of distances to the east. There was also a pronounced lengthening to the south-southwest and the northwest. The shortest 99th percentile of branch distance was 23 km to the east and southeast, and the longest was 34 km to the northwest. A second maximum in the 99th percentile of branch distance was 31 km at 200°. The branch counts were actually higher where the 99th percentile of distance was lower. In fact, the highest branch count of 164,161 was found at 150°, precisely where the minimum distance of 23 km was found. The lowest branch count (139,171) was found to be at 270°. Apparently, branch distance did not depend directly upon branch count during the autumn months. The elongation to the south-southwest may have been a function, again, of orientation of thunderstorms along the sea-breeze boundary.

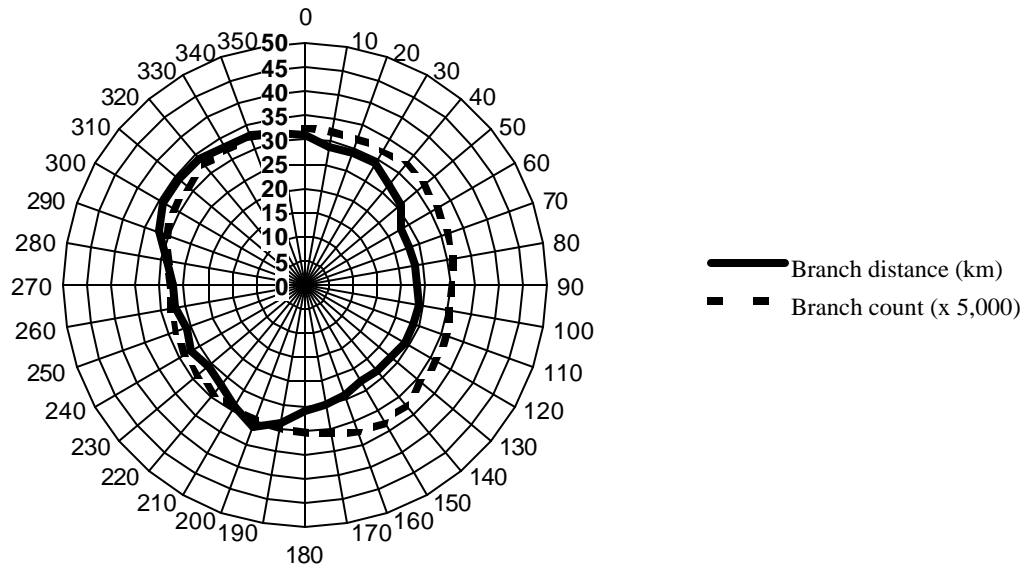


Figure 28. 99th Percentile of Branch Distance by Azimuth for Autumn.

Lastly, the winter plot showed longer 99th percentile distance values than spring and summer. The longest distances were toward the northeast, and there was a significant increase in the branch counts in that direction. The longest 99th percentile of branch distance was 39 km to the north. The shortest values were to the southeast, with a minimum of 25 km at 130°. The most branches (41,115) propagated toward 30°. The smallest branch count was toward 250°, with only 23,527 branches. New cell development to the southwest during cold-frontal passages (which happen most frequently in Florida during the winter) could possibly have yielded the longer and more frequent branches to the north and northeast.

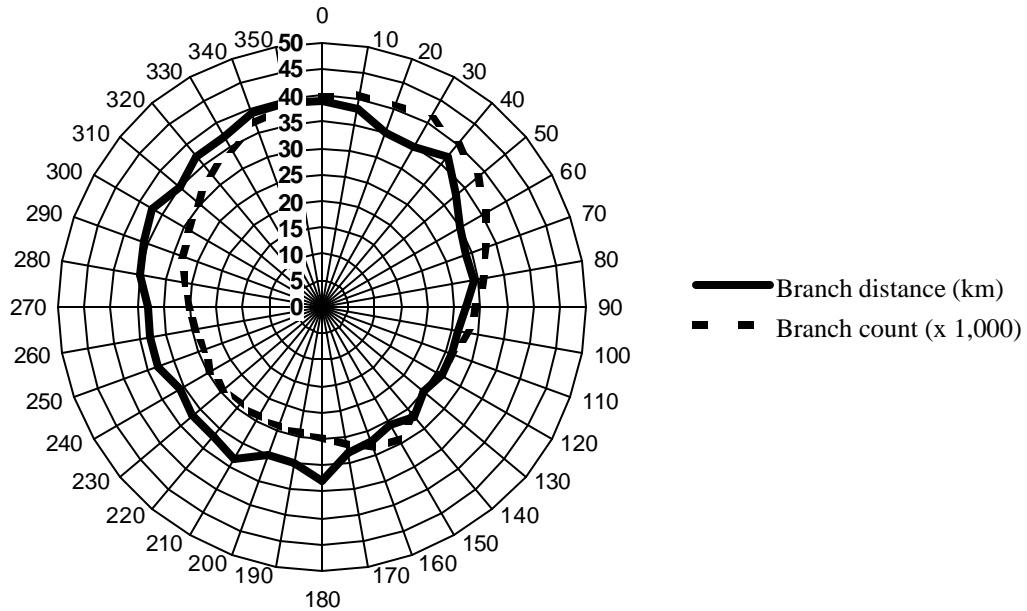


Figure 29. 99th Percentile of Branch Distance by Azimuth for Winter.

Winter and spring seemed to show the strongest azimuthal preference for distance and branch count, while summer showed the least. The influence of synoptic-scale features on thunderstorm alignment and propagation likely had an impact on the horizontal distribution of the cold months. Throughout the warm months, sea breeze fronts oriented along Florida’s east coast as well as those associated with the rivers and lagoons surrounding KSC were also likely to have modified the horizontal orientation of lightning. The usefulness of these results over areas with different geography than KSC is therefore somewhat limited.

V. Conclusions

5.1 Conclusions

The volume of the lightning data examined in this study was quite large. The data were archived from 1 March 1997 to 31 May 2001. The initial data files contained nearly 330 million LDAR data points that were then grouped into sequential lightning flashes and branches using spatial and temporal criteria. Even after reducing the data set to those flashes originating within 60 km of LDAR, there were over 1 million flashes and nearly 40 million branches to study. Some previous studies were limited in scope to single flashes or single storms. Each lightning flash in this study contained anywhere from one branch (the main channel) to the order of tens of branches. Each branch was examined from the parent flash source point to the individual branch end point. Each branch was treated as if it were a single-channel flash, though its source point was considered to be the first point in the entire flash group.

The data appeared to be distributed in an approximately gamma fashion, with the mode value at roughly the 2 km horizontal branch distance. Median branch distance values were typically 4 to 6 km at most vertical levels. The maximum horizontal extent of lightning in this study varied greatly with altitude and distance and was found to be a function of single extreme data points. In an effort to minimize contamination of the data by questionable extremes, the 99th percentile of branch distance was studied in depth. For the entire period of record, the longest branches were found to occur at 2 to 7 km altitude and between 10° and -20°C estimated atmospheric temperature. Within these altitude and temperature ranges, the 99th percentiles of branch distance were roughly 35

to 40 km, with some variation in the vertical. Shorter distances were found above and below the aforementioned temperature range. Distance values were assumed to be the most accurate where branch counts were highest, i.e., from 2 to 15 km altitude. Also, branch count maxima in the flash source altitude and temperature data seemed to correlate well with the expected locations of the upper positive (larger peak) and main negative (smaller peak) regions in the thunderstorm. Branch counts were more evenly distributed in the branch end altitude and temperature data, indicating a slight vertical component to branch propagation. The total period of data showed a difference in distance by azimuth, with the shortest 99th percentile of distance toward the east and southeast.

Stronger relationships between vertical levels and distances were found by season. All four seasons tended to show the same maximum in distance between 2 and 7 km altitude, but the difference between the longer and shorter distance values was more pronounced in autumn than in the other seasons or over the total period. The coldest temperature at which the maximum 99th percentile of distance occurred varied from season to season. In summer, this lower temperature bound was -20°C, but in winter it reached -40°C. This was expected due to the seasonal variation of temperatures at a specific altitude. More importantly, the actual 99th percentile of distance varied from season to season. The winter and spring 99th percentile of branch distance was significantly longer than that for the summer and autumn 99th percentile of distance by all four predictors.

The peak branch count varied in altitude, from 8.7 km in the summer to 7.5 km in the winter. This was likely due to shorter thunderstorm tops in the winter than the

summer. Branch count data also indicated a considerable number of branches in the winter had an upward component.

Horizontal distributions of the seasonal data were then examined. Each season showed a different directional preference for distance as well as branch count. These distributions were likely due to thunderstorm type and line orientation specific to the season and the KSC area. Summer and autumn showed an elongation of distances to the south, indicating that thunderstorms may have been oriented along sea breeze boundaries. Winter and spring data showed a distance elongation and an increased branch count toward the northeast. This result was probably due to the orientation of synoptic-scale fronts passing through the KSC area during these seasons.

5.2 Recommendations

5.2.1 Operator Recommendations. Based on the results of this study, lightning can travel from source regions by distances of 40 km (or roughly 22 nautical miles) in summer and 50 km (27 nautical miles) in winter. Although the longest lightning branches exceeded 100 km (assuming that the data were real and not due to anomalous signal detection or a failure of the flash grouping algorithm), they represented extreme outliers. Quantification of the threat of outlier points is nearly impossible, though often mathematically negligible. Additionally, this study did not address aircraft-induced lightning. Maintaining safe distances from thunderstorms and the strongest electric fields should minimize aircraft charging and the threat of aircraft-induced discharges.

For essential flights in which operators are willing to accept a specific quantifiable threat, the percentiles of distances from flash source to branch end are given

in Appendices A and B. The tables of specific interest to aviators refer to the branch end altitudes and branch end temperatures, respectively, which are more likely to reflect the position of the aircraft (few aircrews will intentionally find themselves within lightning source regions). For example, if one is willing to accept the risk that 5% of the lightning from a storm may reach or exceed one's distance at a flight level of 28,000 feet, one may fly within 20 km of flash source regions, once those regions are identified using radar. Military applications of such a quantified risk assessment may be related to combat or humanitarian requirements.

5.2.2 Future Research Recommendations. The next logical step would be to combine these data with a study of lightning source regions. Locations of lightning flash sources in a thunderstorm from three-dimensional archived weather radar data (in this case, from the Weather Surveillance Radar, 1988 Doppler (WSR-88D) at Melbourne, FL) can be combined with branch distances to give an even better picture of the lightning threat. The research would seek specific knowledge of what reflectivity levels correspond to flash sources. Furthermore, comparisons between on-board aircraft weather radar and WSR-88D data can tell pilots exactly where they can expect lightning to originate, and using this study, can adjust their distance from that reflectivity region accordingly.

Additional studies of CG lightning distances can be combined with these data to verify the threat on the ground from a thunderstorm at various distances. Knowing how far CG flashes can travel from certain radar reflectivity values can aid weather forecasters on the ground in issuing airfield warnings. Categorizing lightning as CG requires

verification by the National Lightning Detection Network, but this study did not differentiate between lightning types.

As more three-dimensional lightning systems become operational, such as the Lightning Mapping System (Kriehbel et al. 1999), more data will be available to determine the degree to which the results of this study were dependent upon local climatology. Data from other parts of the United States as well as the world may show that lightning behaves differently based upon region. Midwestern U.S. data would probably show more synoptically forced thunderstorms than the more typical airmass and sea breeze Florida thunderstorms. A similar study of such a data set would provide valuable information.

More study of the data collected for this project is also possible. While the counting scheme used to build the three-dimensional histogram arrays did not specify which branch end was associated with a specific flash source, that information is available in the form of the flash-grouped LDAR files. These files can be used to determine with more precision the vertical extent of these branches. Specific information of how many branches had a vertical component, their direction, and how much altitude they gained or lost, can give users a better idea of the orientation of the lightning. Intracloud versus cloud-to-air and cloud-to-cloud discharges can be inferred for meteorological interest. The vertical component of otherwise primarily horizontal channels can further clarify the threat to aviators, beyond simply the threat at their specific flight levels.

Appendix A: Percentiles of Distance by Altitude

Lightning data from Kennedy Space Center (KSC) from the period 1 March 1997 to 31 May 2001 were examined to determine the horizontal distance between the flash source points and the end of each branch. Percentiles of lightning branch distance were determined by constructing a cumulative distribution function and calculating the distance value below which the specific percentage of branches fell. Table A-1 shows the percentiles of distance based upon the altitude at which the 1 million lightning flashes and their 39.8 million branches originated. Table A-2 shows the same, except that the distances are based upon the altitude at which the branches terminated.

Table A-1. Percentiles of Branch Distance by Flash Source Altitude.

Altitude (km)	Altitude (feet)	50th Percentile Distance (km)	90th Percentile Distance (km)	95th Percentile Distance (km)	99th Percentile Distance (km)	Maximum Distance (km)
0.0	0	0	0	0	4	16
0.3	984	0	0	0	29	57
0.6	1969	0	2	10	25	57
0.9	2953	0	11	15	26	51
1.2	3937	1	12	16	26	65
1.5	4921	2	12	17	27	59
1.8	5906	4	15	20	35	78
2.1	6890	5	17	22	31	75
2.4	7874	5	17	22	35	90
2.7	8858	5	18	25	41	82
3.0	9843	5	17	23	38	93
3.3	10827	5	17	23	39	87
3.6	11811	5	18	24	40	118
3.9	12795	5	18	24	40	111
4.2	13780	5	17	22	37	101
4.5	14764	5	17	23	36	112
4.8	15748	5	17	22	38	117
5.1	16732	5	17	22	37	120
5.4	17717	5	17	22	38	128
5.7	18701	5	16	22	37	131
6.0	19685	5	16	22	38	147
6.3	20669	5	17	23	37	142
6.6	21654	5	17	23	38	122
6.9	22638	6	17	23	40	127
7.2	23622	5	16	22	36	96
7.5	24606	5	16	21	35	103

Appendix A: Percentiles of Distance by Altitude (cont.)

Table A-1 (cont.). Percentiles of Branch Distance by Flash Source Altitude.

Altitude (km)	Altitude (feet)	50th Percentile Distance (km)	90th Percentile Distance (km)	95th Percentile Distance (km)	99th Percentile Distance (km)	Maximum Distance (km)
7.8	25591	5	15	21	34	164
8.1	26575	5	15	20	34	147
8.4	27559	4	14	19	32	154
8.7	28543	4	14	19	32	123
9.0	29528	4	14	19	31	125
9.3	30512	4	13	18	30	107
9.6	31496	4	14	18	30	134
9.9	32480	4	13	18	29	102
10.2	33465	4	14	18	31	118
10.5	34449	4	14	18	29	112
10.8	35433	4	14	19	30	105
11.1	36417	4	14	18	30	108
11.4	37402	5	14	18	31	104
11.7	38386	5	14	18	29	100
12.0	39370	5	14	19	30	99
12.3	40354	5	15	19	31	122
12.6	41339	5	15	19	30	87
12.9	42323	5	14	19	30	136
13.2	43307	5	14	19	29	96
13.5	44291	5	14	19	30	116
13.8	45276	5	14	19	30	97
14.1	46260	5	14	17	28	103
14.4	47244	5	14	18	28	95
14.7	48228	6	15	19	30	115
15.0	49213	6	14	18	29	104
15.3	50197	6	14	18	27	76
15.6	51181	6	14	17	29	85
15.9	52165	6	14	18	26	58
16.2	53150	6	15	18	26	49
16.5	54134	7	16	20	30	104
16.8	55118	7	16	20	30	74
17.1	56102	7	16	20	26	53
17.4	57087	7	16	20	26	45
17.7	58071	6	16	20	29	63
18.0	59055	7	14	16	20	27
18.3	60039	8	15	18	23	34
18.6	61024	8	18	27	35	65
18.9	62008	8	17	21	26	29
19.2	62992	10	19	23	33	47
19.5	63976	8	17	23	28	34
19.8	64961	10	21	30	33	35
20.1	65945	8	15	16	21	28
20.4	66929	10	16	17	19	28
20.7	67913	10	21	24	26	41
21.0	68898	11	29	31	33	34

Appendix A: Percentiles of Distance by Altitude (cont.)

Table A-1 (cont.). Percentiles of Branch Distance by Flash Source Altitude.

Altitude (km)	Altitude (feet)	50th Percentile Distance (km)	90th Percentile Distance (km)	95th Percentile Distance (km)	99th Percentile Distance (km)	Maximum Distance (km)
21.3	69882	13	22	24	27	29
21.6	70866	10	17	20	25	25
21.9	71850	16	21	23	28	35
22.2	72835	8	12	15	18	18
22.5	73819	17	23	24	25	27
22.8	74803	6	11	15	26	26
23.1	75787	10	13	14	14	14
23.4	76772	8	10	10	11	11
23.7	77756	4	7	7	7	7
24.0	78740	8	12	14	17	20
24.3	79724	10	17	20	24	24
24.6	80709	7	16	17	18	18
24.9	81693	11	14	15	18	18
25.2	82677	15	20	21	22	23
25.5	83661	12	16	19	19	19

Appendix A: Percentiles of Distance by Altitude - (cont.)

Table A-2. Percentiles of Branch Distance by Branch End Point Altitude.

Altitude (km)	Altitude (feet)	50th Percentile Distance (km)	90th Percentile Distance (km)	95th Percentile Distance (km)	99th Percentile Distance (km)	Maximum Distance (km)
0.0	0	0	0	0	5	51
0.3	984	0	0	3	9	74
0.6	1969	0	4	7	17	78
0.9	2953	0	8	12	23	78
1.2	3937	2	11	16	29	80
1.5	4921	2	12	17	31	118
1.8	5906	4	13	19	34	129
2.1	6890	5	15	21	37	123
2.4	7874	5	15	21	37	119
2.7	8858	5	16	22	38	121
3.0	9843	5	16	22	38	138
3.3	10827	5	17	23	38	126
3.6	11811	5	17	23	39	131
3.9	12795	5	17	23	38	121
4.2	13780	5	17	23	38	121
4.5	14764	5	17	23	38	120
4.8	15748	5	17	23	37	130
5.1	16732	5	17	22	37	121
5.4	17717	5	17	22	37	130
5.7	18701	5	16	22	36	127
6.0	19685	5	16	21	36	130
6.3	20669	5	16	21	35	135
6.6	21654	5	15	21	35	138
6.9	22638	5	15	20	34	140
7.2	23622	5	15	20	34	133
7.5	24606	5	15	20	34	147
7.8	25591	5	15	20	34	132
8.1	26575	5	14	20	34	121
8.4	27559	4	14	20	34	142
8.7	28543	4	14	19	33	119
9.0	29528	4	14	19	33	111
9.3	30512	4	14	19	32	125
9.6	31496	4	14	19	32	144
9.9	32480	4	14	19	31	122
10.2	33465	4	14	19	31	112
10.5	34449	4	14	19	31	164
10.8	35433	4	14	18	30	154
11.1	36417	4	14	18	30	110
11.4	37402	5	14	19	30	131
11.7	38386	5	14	19	30	108
12.0	39370	5	14	19	30	116
12.3	40354	5	14	19	30	110
12.6	41339	5	14	19	30	108
12.9	42323	5	14	19	30	129

Appendix A: Percentiles of Distance by Altitude - (cont.)

Table A-2 (cont.). Percentiles of Branch Distance by Branch End Point Altitude.

Altitude (km)	Altitude (feet)	50th Percentile Distance (km)	90th Percentile Distance (km)	95th Percentile Distance (km)	99th Percentile Distance (km)	Maximum Distance (km)
13.2	43307	5	14	19	30	105
13.5	44291	5	14	19	30	113
13.8	45276	5	14	19	30	122
14.1	46260	5	15	19	30	109
14.4	47244	5	15	19	30	133
14.7	48228	5	15	19	31	103
15.0	49213	6	15	20	31	120
15.3	50197	6	16	20	32	142
15.6	51181	6	16	21	33	126
15.9	52165	6	17	22	34	110
16.2	53150	7	18	23	35	136
16.5	54134	7	19	24	37	104
16.8	55118	8	20	25	38	138
17.1	56102	9	21	26	40	141
17.4	57087	10	22	27	41	154
17.7	58071	10	23	28	43	103
18.0	59055	11	23	28	44	162
18.3	60039	11	24	30	45	101
18.6	61024	12	25	30	44	102
18.9	62008	12	25	31	47	111
19.2	62992	13	26	32	48	99
19.5	63976	14	27	33	50	82
19.8	64961	14	28	34	49	97
20.1	65945	14	28	34	51	131
20.4	66929	15	28	34	49	87
20.7	67913	15	29	35	50	104
21.0	68898	16	29	35	51	97
21.3	69882	16	29	35	50	93
21.6	70866	17	31	39	56	103
21.9	71850	17	32	37	52	147
22.2	72835	18	33	38	53	111
22.5	73819	18	32	38	59	90
22.8	74803	18	34	41	59	92
23.1	75787	18	34	40	58	97
23.4	76772	19	36	43	58	74
23.7	77756	20	38	45	73	131
24.0	78740	21	36	44	60	80
24.3	79724	20	36	41	54	80
24.6	80709	21	35	41	64	80
24.9	81693	21	37	42	61	92
25.2	82677	19	38	45	59	64
25.5	83661	19	40	43	81	81

Appendix B: Percentiles of Distance By Temperature

Lightning data from Kennedy Space Center (KSC) from the period 1 March 1997 to 31 May 2001 were examined to determine the horizontal distance between the flash source points and the end of each branch. Percentiles of branch distance were determined by constructing a cumulative distribution function and calculating the distance value below which the specific percentage of branches fell. Table B-1 shows the percentiles of distance based upon the estimated atmospheric temperature (interpolated from rawinsonde data) at which the 1 million lightning flashes and their 39.8 million branches originated. Table B-2 shows the same, except that the distances are based upon the estimated atmospheric temperature at which the branches terminated.

Table B-1. Percentiles of Branch Distance by Flash Source Temperature.

Temperature (C)	Temperature (F)	50th Percentile Distance (km)	90th Percentile Distance (km)	95th Percentile Distance (km)	99th Percentile Distance (km)	Maximum Distance (km)
-80	-112	5	12	14	20	129
-78	-108	5	12	17	27	105
-76	-105	5	12	16	24	113
-74	-101	6	14	17	27	122
-72	-98	6	15	20	31	109
-70	-94	6	16	20	32	133
-68	-90	5	15	19	29	103
-66	-87	5	14	18	29	120
-64	-83	5	14	19	29	142
-62	-80	5	14	19	30	126
-60	-76	5	15	19	31	110
-58	-72	5	15	19	31	136
-56	-69	5	15	19	31	104
-54	-65	5	14	19	30	138
-52	-62	5	14	19	31	141
-50	-58	5	15	19	32	154
-48	-54	5	14	19	31	103
-46	-51	5	14	19	31	162
-44	-47	4	14	18	29	101
-42	-44	4	14	19	30	102
-40	-40	4	14	18	30	111
-38	-36	4	14	19	31	99
-36	-33	4	14	19	31	82
-34	-29	4	14	19	32	97

Appendix B: Percentiles of Distance By Temperature (cont.)

Table B-1 (cont.). Percentiles of Branch Distance by Flash Source Temperature.

Temperature (C)	Temperature (F)	50th Percentile Distance (km)	90th Percentile Distance (km)	95th Percentile Distance (km)	99th Percentile Distance (km)	Maximum Distance (km)
-32	-26	4	14	19	32	131
-30	-22	4	14	19	32	87
-28	-18	4	14	19	32	104
-26	-15	4	14	19	32	97
-24	-11	5	15	20	33	93
-22	-8	5	15	20	33	103
-20	-4	5	16	21	35	147
-18	0	5	16	22	36	111
-16	3	5	17	23	39	90
-14	7	5	17	23	39	92
-12	10	5	17	22	37	97
-10	14	5	17	22	38	74
-8	18	5	16	22	37	131
-6	21	5	17	22	37	80
-4	25	5	17	22	37	80
-2	28	5	16	22	36	80
0	32	5	17	22	37	92
2	36	5	17	22	38	64
4	39	5	17	23	38	81
6	43	5	15	21	35	85
8	46	5	16	21	35	90
10	50	4	16	20	31	73
12	54	4	16	21	36	78
14	57	3	13	18	26	47
16	61	3	12	16	25	65
18	64	0	10	15	26	58
20	68	0	8	13	27	56
22	72	0	6	12	24	57
24	75	0	0	2	30	57
26	79	0	2	13	25	29
28	82	0	0	1	4	9
30	86	0	0	0	0	0
32	90	0	0	0	0	0
34	93	0	0	0	0	0
36	97	0	0	0	0	0
38	100	0	0	0	0	0
40	104	0	0	0	0	0

Appendix B: Percentiles of Distance By Temperature (cont.)

Table B-2. Percentiles of Branch Distance by Branch End Point Temperature.

Temperature (C)	Temperature (F)	50th Percentile Distance (km)	90th Percentile Distance (km)	95th Percentile Distance (km)	99th Percentile Distance (km)	Maximum Distance (km)
-80	-112	5	14	18	29	113
-78	-108	5	13	17	28	109
-76	-105	5	14	18	29	120
-74	-101	6	15	20	31	120
-72	-98	6	17	21	34	154
-70	-94	6	16	21	34	142
-68	-90	6	16	20	33	162
-66	-87	5	15	19	31	123
-64	-83	6	15	20	32	131
-62	-80	5	15	19	31	147
-60	-76	5	15	20	32	129
-58	-72	5	15	19	30	112
-56	-69	5	15	19	31	103
-54	-65	5	14	19	30	154
-52	-62	5	14	19	30	125
-50	-58	5	15	20	31	131
-48	-54	5	14	19	31	112
-46	-51	5	14	19	31	164
-44	-47	4	14	18	30	104
-42	-44	4	14	19	31	125
-40	-40	4	14	19	31	122
-38	-36	4	14	19	33	144
-36	-33	4	14	19	32	128
-34	-29	4	14	19	33	142
-32	-26	4	14	20	34	119
-30	-22	4	14	19	33	119
-28	-18	4	14	20	34	140
-26	-15	4	14	20	34	128
-24	-11	4	15	20	34	135
-22	-8	4	15	20	33	126
-20	-4	4	15	20	33	147
-18	0	5	15	20	34	134
-16	3	5	15	20	34	140
-14	7	5	15	20	34	132
-12	10	5	16	21	35	135
-10	14	5	16	21	36	130
-8	18	5	16	21	35	126
-6	21	5	17	22	36	130
-4	25	5	17	23	37	121
-2	28	5	17	22	37	131
0	32	5	17	23	38	127
2	36	4	16	21	36	125
4	39	4	16	21	36	126
6	43	4	15	21	36	138
8	46	4	15	20	36	120

Appendix B: Percentiles of Distance By Temperature (cont.)

Table B-2 (cont.). Percentiles of Branch Distance by Branch End Point Temperature.

Temperature (C)	Temperature (F)	50th Percentile Distance (km)	90th Percentile Distance (km)	95th Percentile Distance (km)	99th Percentile Distance (km)	Maximum Distance (km)
10	50	4	14	19	35	123
12	54	4	13	18	34	103
14	57	3	12	17	31	129
16	61	3	11	16	30	106
18	64	2	9	13	24	80
20	68	0	8	11	21	78
22	72	0	5	8	17	75
24	75	0	3	5	13	74
26	79	0	6	9	18	32
28	82	0	0	2	8	19
30	86	3	10	10	10	10
32	90	0	0	0	0	0
34	93	0	0	0	0	0
36	97	0	0	0	0	0
38	100	0	0	0	0	0
40	104	0	0	0	0	0

Bibliography

- Berger, K. and E. Vogelsanger, 1966. Photographische Blitzuntersuchungen der Jahre 1955...1965 auf dem Monte San Salvatore. *Bull. Schweiz. Elektrotech. Ver.*, **57**, 599-620.
- Bluestein, H. B., 1992: *Synoptic-Dynamic Meteorology in Midlatitudes Volume 1: Principles of Kinematics and Dynamics*. Oxford University Press, 430 pp.
- Boccippio, D. J., S. Heckman, S. J. Goodman, 2001: A Diagnostic Analysis of the Kennedy Space Center LDAR Network, 1. Data Characteristics. *J. Geophys. Res.*, **106**, 4769-4786.
- Department of the Air Force. *Lightning Protection*. T.O. 1C-17A-ISS-91. Wright-Patterson AFB, OH: ASC/YC, 17 July 2001.
- Engholm, C. D., E. R. Williams, and R. M. Dole, 1990: Meteorological and electrical conditions associated with positive cloud-to-ground lightning. *Mon. Wea. Rev.*, **118**, 470-487.
- Glickman, T. S., Ed., 2000: *Glossary of Meteorology*. Amer. Meteor. Soc., 855 pp.
- Krehbiel, R. J., R. J. Thomas, W. Rison, T. Hamlin, J. Harlin, M. Davis, 1999: Three-Dimensional lightning mapping observations during MEaPRS in central Oklahoma. *Proc. 11th Int. Conf. on Atmos. Electricity*, Guntersville, AL, National Aeronautics and Space Administration, 376-379.
- Krider, E. P., M. J. Murphy, D. W. Schiber, and L. M. Maier, 1996: The Electrical Structure of Florida Thunderstorms. *Proc. 10th Int. Conf. on Atmos. Electricity*. Osaka, Japan, Soc. Of Atmospheric Electricity of Japan, 124-125.

- Laroche, P., A. Bondiou, P. Blanchet, M. Weber, and B. Boldi, 1996. 3D Structure of Lightning Discharge Within Storms. *Proc. 10th Int. Conf. on Atmos. Electricity*. Osaka, Japan, Soc. Of Atmospheric Electricity of Japan, 329-332.
- Lennon, C. and L. Maier, 1991: Lightning mapping system. *Proc. Int. Aerospace and Ground Conf. on Lightning and Static Electricity*. Cocoa Beach, FL, NASA, 89-1 - 89-10.
- MacGorman, D. R. and W. D. Rust, 1998: *The Electrical Nature of Storms*. Oxford University Press, 422 pp.
- Maier, L., C. Lennon, P. Krehbiel, and M. Maier, 1996. Lightning as observed by a four-dimensional lightning location system at Kennedy Space Center. *Proc. 10th Int. Conf. on Atmos. Electricity*. Osaka, Japan, Soc. Of Atmospheric Electricity of Japan, 280-283.
- Murphy, M., K. Cummins, and L. Maier, 2000. The analysis and interpretation of three-dimensional lightning flash information. *Proc. 80th Amer. Meteor. Soc. Meeting*, Long Beach, CA.
- NASA, cited 2001: Build_flash_v6.c. [Available on-line from http://kscdl2.ksc.nasa.gov/public/ldar/build_flash_v6.c]
- Ogawa, T. and M. Brook, 1964. The mechanism of the intracloud lightning discharge. *J. Geophys. Res.*, **69**, 5141-5150.
- Phelps, C. T., 1974. Positive streamer system intensification and its possible role in lightning initiation. *J. Atmos. Terr. Phys.*, **36**, 103-111.
- Prentice, S. A. and D. Mackerras, 1977. The ratio of cloud to cloud-ground lightning flashes in thunderstorms. *J. Appl. Meteor.*, **16**, 545-550.

Shao, X. M. and P. Krehbiel, 1996. The spatial and temporal development of intracloud lightning. *Proc. 10th Int. Conf. on Atmos. Electricity*. Osaka, Japan, Soc. Of Atmospheric Electricity of Japan, 321-322.

Stolzenburg, M, D. W. Rust, and T. C. Marshall, 1998: Electrical structure in thunderstorm convective regions. 3. Synthesis. *J. Geophys. Res.*, **103**, 14,097-14,108.

Uman, M. A., 2001: *The Lightning Discharge*. Dover Publications, 377 pp.

Wilks, D S., 1995: *Statistical Methods in the Atmospheric Sciences*. Academic Press, 464 pp.

Vita

Captain David R. Vollmer graduated with a Bachelor of Science degree in meteorology from the Pennsylvania State University in January, 1996. He received an appointment to the U.S. Air Force Officer Training School, where he was commissioned in June 1996.

Capt Vollmer's first duty assignment was to the 21st Air Support Operations Squadron at Fort Polk, LA. There he performed staff weather officer duties with the Joint Readiness Training Center. During the winter of 1997-98 he deployed to Bosnia-Herzegovina with Task Force Eagle as part of the Operation JOINT GUARD peacekeeping mission. In April 1998, he was assigned to the 607th Weather Squadron (WS) in Seoul, Republic of Korea. There he spent a year as weather programs officer and another year as the 17th Aviation Brigade staff weather officer, as well as the Officer-in-Charge of Operating Location A, 607th WS. Capt Vollmer entered the Graduate School of Engineering and Management, Air Force Institute of Technology, in August, 2000. Upon graduation, he will be assigned to the Air Force Technical Applications Center at Patrick AFB, FL.

REPORT DOCUMENTATION PAGE

*Form Approved
OMB No. 0704-0188*

The public reporting burden for this collection of information is estimated to average 1 hour per response, including the time for reviewing instructions, searching existing data sources, gathering and maintaining the data needed, and completing and reviewing the collection of information. Send comments regarding this burden estimate or any other aspect of this collection of information, including suggestions for reducing the burden, to Department of Defense, Washington Headquarters Services, Directorate for Information Operations and Reports (0704-0188), 1215 Jefferson Davis Highway, Suite 1204, Arlington, VA 22202-4302. Respondents should be aware that notwithstanding any other provision of law, no person shall be subject to any penalty for failing to comply with a collection of information if it does not display a currently valid OMB control number.

PLEASE DO NOT RETURN YOUR FORM TO THE ABOVE ADDRESS.

1. REPORT DATE (DD-MM-YYYY) 26-03-2002		2. REPORT TYPE Master's Thesis		3. DATES COVERED (From - To) Jun 2001-Mar 2002	
4. TITLE AND SUBTITLE THE HORIZONTAL EXTENT OF LIGHTNING BASED ON ALTITUDE AND ATMOSPHERIC TEMPERATURE				5a. CONTRACT NUMBER	
				5b. GRANT NUMBER	
				5c. PROGRAM ELEMENT NUMBER	
6. AUTHOR(S) Vollmer, David R., Captain, USAF				5d. PROJECT NUMBER	
				5e. TASK NUMBER	
				5f. WORK UNIT NUMBER	
7. PERFORMING ORGANIZATION NAME(S) AND ADDRESS(ES) Air Force Institute of Technology Graduate School of Engineering and Management (AFIT/EN) 2950 P Street, Building 640 WPAFB OH 45433-7765				8. PERFORMING ORGANIZATION REPORT NUMBER AFIT/GM/ENP/02M-10	
9. SPONSORING/MONITORING AGENCY NAME(S) AND ADDRESS(ES) ASC/YCA ATTN: Lt Col Robert S. Baerst 2690 Loop Road West WPAFB, OH 45433				10. SPONSOR/MONITOR'S ACRONYM(S)	
				11. SPONSOR/MONITOR'S REPORT NUMBER(S) DSN: 986-9419 e-mail: Steve.Baerst@wpafb.af.mil	
12. DISTRIBUTION/AVAILABILITY STATEMENT APPROVED FOR PUBLIC RELEASE; DISTRIBUTION UNLIMITED.					
13. SUPPLEMENTARY NOTES					
14. ABSTRACT Lightning poses a threat to aircraft in flight. To mitigate this threat, the U.S. Air Force requested a study of lightning distances. Three-dimensional lightning data were examined for this study, spanning 1 March 1997 to 31 May 2001 and obtained from the Lightning Detection and Ranging System (LDAR) at the Kennedy Space Center, FL. The LDAR data points were first grouped into lightning flashes and branches using spatial and temporal criteria. Rawinsonde data were vertically interpolated to determine the temperature at the flash source point and each branch end point. The horizontal distance from flash source to branch end was calculated. Percentiles of branch distance were examined as a function of altitude and temperature of the flash source and branch end points. The longest 99th percentile of branch distance (35 to 40 km) was found at 2 to 7 km altitude and between 10 and -20C. The altitude range of the longest branches remained similar by season, but the longest branches were found in the winter and spring months, with summer and autumn distances shorter by 5 to 10 km. Summer results showed longer branch distances to the south and the winter data showed a significant elongation to the north.					
15. SUBJECT TERMS Lightning, Atmospheric Electricity, Lightning Protection, Electric Discharges					
16. SECURITY CLASSIFICATION OF:			17. LIMITATION OF ABSTRACT UU	18. NUMBER OF PAGES 80	19a. NAME OF RESPONSIBLE PERSON Vollmer, David R., Captain, USAF (ENP)
a. REPORT U	b. ABSTRACT U	c. THIS PAGE U			19b. TELEPHONE NUMBER (Include area code) (937) 255-3636 ext 6316, david.vollmer@afit.edu

